공학박사학위논문

효율적인 전역 최적해 탐색을 위한 천음속 축류 압축기의 복합 다분야 통합 최적설계 프레임워크 개발

Hybrid Framework Construction of Multidisciplinary Design Optimization for Transonic Axial Compressor with Efficient Global Optimum Exploration

2013 년 8 월

서울대학교 대학원
기계항공공학부
이 세 일

효율적인 전역 최적해 탐색을 위한 천음속 축류 압축기의 복합 다분야 통합 최적설계 프레임워크 개발

Hybrid Framework Construction of Multidisciplinary Design Optimization for Transonic Axial Compressor with Efficient Global Optimum Exploration

지도교수 이 동 호

이 논문을 공학박사 학위논문으로 제출함

2013 년 8 월

서울대학교 대학원

기계항공공학부

이 세 일

이세일의 공학박사 학위논문을 인준함

2013 년 8 월

위 원 장 : _____

부위원장 : _____

위 원 : _____

위 원 : _____

위 원 : _____

Abstract

Hybrid Framework Construction of Multidisciplinary Design Optimization for Transonic Axial Compressor with Efficient Global Optimum Exploration

Saeil Lee
School of Mechanical and Aerospace Engineering
Seoul National University

Design optimization of aircraft turbo engine compressor is performed with Multidisciplinary Design Optimization (MDO) since it commonly has very complex shapes and its stability characteristics are very difficult to fully analyze. Furthermore, Optimization Results gained by approximation model have an error compared to numerical analysis data. If these optimum data were used for manufacturing and examination, there could be a difference between the expectation and the real value. In this research, development of multidisciplinary design optimization framework is done to apply the optimum result not only qualitatively but also quantitatively manufacturing for transonic axial compressor. To make the framework more efficiently and secure the global optimum, approximation model is adopted and genetic algorithm is used for finding global optimum solution. However, approximation model has implicit error in constructed model. For that reason, the hybrid optimization framework is constructed. Hybrid optimization framework means that two different optimization techniques are combined and simultaneously work in one optimization process. This framework consists of two steps. First step is global optimum searching step using

approximation mode and second step is finding accurate optimum result using gradient based searching method. In second step, during searching the optimum point, approximation model is not applied and numerical analysis is done directly in every steps of searching. To validate the framework and analysis tools, real scale transonic low pressure compressor rotor and stator was manufactured and tested in test rig with result of constructed optimization framework. Compressor test was done by KARI. The objective function of optimization is aerodynamic efficiency and safety factor for structural stability. The efficiency is increased 2.1% point and the safety factor is increased 217%. But this result has narrow operating section because of small stall margin. To secure the stable operating domain, diffusion factor is added to objective function. Minimize the diffusion factor expects loss diminution and stall margin extension. As a result, the stall margin is broadened 19.7% with enhanced aerodynamic efficiency by 4.49% and safety factor by 13.6%. As a result, using the hybrid multidisciplinary design optimization framework for axial compressor which suggested in this work approve the accuracy between the optimum result and the numerical analysis result with the improvement of performances.

Key Words: Multidisciplinary Design Optimization, Transonic Axial Low Pressure Compressor, Approximation Model, Double Step Optimization, Gradient Based Method, Diffusion Factor.

Student Number: 2009-20706

Table of Contents

Nomenclatures

English Symbols

ANN	artificial neural network
c	absolute velocity in velocity triangle diagram
C	chord length
DF	diffusion factor
DOE	design of experiment
k	specific heat of air
$\dot{m}$	mass flow rate
PR	pressure ratio
S	solidity
SF	safety factor
SM	stall margin
w	relative velocity in velocity triangle diagram

Greek Symbols

β_1	inlet angle
β_2	outlet angle
η	efficiency
σ	calculated maximum stress of the compressor
σ_Y	yield stress of the compressor

Subscripts

0	factor of the initial shape, isentropic coefficient
1-5	section number of design variable in rotor blade
ad	adiabatic

List of Tables

List of Figures

Chapter 1. Introduction

1.1 Motivations

Axial Compressors are widely applied to modern gas turbine engines and as a spin-off technology, they are also utilized for numerous industries such as large capacity air or gas transportation systems, gas turbine for the plants, air conditioning, refrigeration systems and so on. Most recently demand for light and small but highly loaded compressors is increasing. Therefore, it is necessary to employ state-of-the-art compressor design technology to development of highly loaded efficient compressors. Generally compressor designs are carried out based on experimental data and corresponding empirical formulas. A compressor has to satisfy design requirements such as the mass flow, pressure ratio and efficiency from engine cycle analysis and guarantee wide stable operating ranges to protect compressor from instability. The process of compressor development usually consists of three steps. The first step is to define the design requirements and design variables, the second is compressor sizing and design of detailed flow path and airfoils, and the last step is to assess the compressor aerodynamic performance and structural stability and iterate design revisions in order to determine the final compressor design.

For many years, various compressor design optimization technologies have been researched to improve the performance of compressors. Lee et al. optimized compressor blades for better aerodynamic efficiency with 2nd order response surface method [1]. Benini used a multi-objective evolutionary algorithm to optimize the blades of a compressor using CFX with a multi-objective function which was consisted of adiabatic efficiency and total-to-

total pressure ratio [2]. Samad and Kim developed an optimization technique using response surface model to improve adiabatic efficiency and total pressure ratio [3]. Lee et al. also used response surface method to design axial fan to achieve better aerodynamic efficiency and pressure ratio [4]. Chen et al. [5] applied the efficiency for objective function in compressor design optimization. And Keskin and Bestle developed axial compressor preliminary design optimization method for maximize polytropic efficiency, pressure ratio and surge margin subject to initial aerodynamic characteristics [6]. These studies focused on only aerodynamic improvements. Furthermore, the stall margin (SM) of the compressor is too complex to be analyzed fully by numerical methods. In addition, it is an important factor for stable operation of the aircraft compressor when the aircraft is in flight. Choi [7] adopted SM as a factor for a multi-objective function, but they assumed that the pressure ratio and the mass flow rate at the stall point could be calculated precisely by numerical analysis by CFD or via a commercial program. However, SM is influenced by the flow conditions at the stall point and the initial point; thus, it is difficult to detect these conditions accurately by the unstable properties of the stall state as the compressor operates. For this reason, the Lieblein diffusion factor (DF) is used for estimation of SM in this work [8],[9]. Meanwhile, Leyens et al. optimized a compressor blade to reduce the weight of the compressor [10]. This study defined the objective function for only a structural topic. These early studies on aerodynamic or structural optimizations revealed that design shape for a better aerodynamic performance is generally in conflict with design shape for more stable structure. As a result, during the design process of highly loaded axial compressor, these inconsistencies have to make compromise between aerodynamic performance and structural characteristics. In other words,

various design requirements of compressor must be balanced by considering characteristics of subsystems such as the aerodynamic and structural characteristics, respectively. In this manner, the multidisciplinary design optimization (MDO) method, which considers various subsystems simultaneously throughout the design process, is considered to be a very effective tool for the design of the types of compressor.

Recently, MDO technologies have been successfully applied to compressor design optimizations while mostly combining two disciplines; aerodynamics and structure. Lim and Chung [11] used combination of efficiency and weight of the compressor and Lian and Liou [12] integrated pressure ratio and weight for a multi-objective function. Pierret et al. [13] integrated efficiency and Von Mises stress of the compressor. And Chen et al. [14] combined pressure ratio, stall margin and weight as a multi-objective function. These researches had successfully combined these two disciplines of the aircraft compressor design optimization problems and improved each factor of the multi-objective functions.

To improve the design process of compressors, study on development of pertinent compressor MDO design framework is required so that the compressor development cycles can be reduced, while ensuring reliability of design results. However, the development of a feasible MDO framework, which can predict accurate nonlinear responses of compressor design variable, is too difficult to be achieved easily. Oyama and Liou used multi-objective optimization technique using evolutionary algorithm for rocket engine pumps without approximation model and this method require numerical analysis at every step [15]. It can only apply to problem with simple computation analysis. The present study requires lots of computational time to get a numerical analysis result. Consequently, this study has to construct the

optimization framework with a surrogated model. Hong et al. developed optimization techniques for axial compressor to improve aerodynamic and structural characteristics with artificial neural network approximation method [16],[17]. But these results had an accuracy problem between surrogated model results and CFD results.

For this reason, in the present study, a concept of hybrid MDO framework is developed. It has double-step multi-objective optimizer in one framework. This framework consists of a gradient based optimization method, starting from the global optimum point obtained from approximation model. Approximation model is constructed using an artificial neural network with experimental points form design of experiment process. The genetic algorithm is used for finding the global optimum point and sequential quadratic programming algorithm is used for finding final optimal result. Aerodynamic and structural performances of axial compressor for optimization process are evaluated by using commercial codes. The results from the numerical analysis are validated with experimental results from the compressor test facility.

1.2 Background and Previous Researches

1.2.1. Axial Compressor

The axial compressor is a part of the turbofan engine or the gas turbine shown as Fig. 1.1 [17]. In the turbofan engine, reaching the target pressure ratio in a single compressor stage is a difficult job. In this reason, a typical axial compressor consists of many stages. And an each stage has a rotating row, called rotor blades and stationary part, called stator blades. In Fig. 1.2 [18], a typical axial compressor passage is illustrated. The rotor row gives

work to the working fluid and it accelerates the fluid. Then passing through the stator row, the fluid is decelerated. This deceleration changes the kinetic energy which gained by rotor blades to the static pressure with the stagnation temperature remaining constant. This basic operation was done in an each stage. The stagnation pressure is increased within the rotor row. And in real world, there are some losses due to fluid friction in the stator row. These losses decrease the stagnation pressure. A T-s diagram for the stage is shown in Fig. 1.3.[19]

The process is then repeated as many times as necessary to get the required pressure ratio. However, an each stage makes the compressor heavy and long. Weight of the compressor should be decreased for the efficient performance of the aircraft engine. To reduce the weight, the number of compressor stage and the number of compressor blades must be decreased. These weight reduction techniques burden on the compressor blade. To make the required blade loading on compressor blades, the rotating speed should be increased. Fast rotating speed causes the structural problem. And it also causes shock wave due to enter the transonic region. There are some losses near shock wave. History of the compressor development is shown in table 1.1 [22]

1.2.2 Compressor Aerodynamic characteristics

The velocity diagrams for the stage are shown in Fig. 1.4 [20]. It is expressed in absolute and relative velocity vectors. In a typical compressor stage, absolute velocities and flow directions at stage inlet and outlet are the same. The flow from a previous stage to the rotor row has an absolute velocity c_1, and direction α_1. And rotation speed U gives the inlet relative velocity w_1

and direction β_1. When passing through the rotor row, the working fluid gets kinetic energy from the rotating blade. At the outlet of rotor row, absolute velocity c_2 is increased than c_1. And relative to the rotor blades, the flow is turned to the angle of β_2 with relative velocity w_2. By vectorially adding the blade speed U onto w_2 gives the absolute velocity c_2 and direction α_2. The stator row pivots the flow angle to the α_3 and the exit velocity is c_3.

- **Adiabatic Efficiency**

The adiabatic efficiency is defined as ratio between adiabatic enthalpy increase ΔH_{ad} and the actual enthalpy increase after the compressor ΔH[21]. It is shown in eq. (1.1)

$$\eta_{ad} = \frac{\Delta H_{ad}}{\Delta H} = \frac{T_1((^{P_2}/_{P_1})^{\frac{k-1}{k}} - 1)}{T_2 - T_1} \qquad (1.1)$$

Where k is a specific heat of air at constant volume and it is a constant 1.4.

1.3 Dissertation Objectives & Outline

This study proposes a hybrid MDO framework for aerodynamic-structural design optimization of the transonic axial compressor for small aircraft engines. The results of compressor design optimization are enhanced according to first step of MDO framework using approximation model. To achieve the reliable results, optimization with gradient based method is done and numerical analysis is done during every searching step in second step of MDO framework.

To achieve these objectives, this paper is organized in the following order. At first, introduction about this study is presented in Chapter 1, and MDO and hybrid double-step optimization techniques (e.g. sensitivity analysis, D-optimal design, ANN, Kriging etc.) used in this study are explained in Chapter 2. The process of aircraft turbo engine compressor MDO framework for composing aerodynamics and structure disciplines is presented in Chapter 3. The comparison between MDO and double-step MDO is suggested in this chapter. This chapter also introduces all the matters about the construction of MDO framework for aircraft turbo engine compressor from the objective function to the details of MDO such as the approximation modeling, the design of experiment method, etc. In Chapter 4, it is explained that MDO process for securing stall margin with controlling the diffusion factor for an object in the multi-objective function. The improved results and stall margin are discussed by comparing the optimized results in Chapter 4. Finally, the overall conclusions and future works are suggested in the last chapter, Chapter 5.

Table 1. 1 History of compressor development by General Electric [22]

Year	Designation	Design Pressure ratio	Number of stages	Corrected tip speed (m/s)
Late 50s	CJ805/J79	12.5	17	291
1969	CF6-50	13.0	14	360
1974	CFM56	12	9	396
1982	E^3 engine	23	10	456

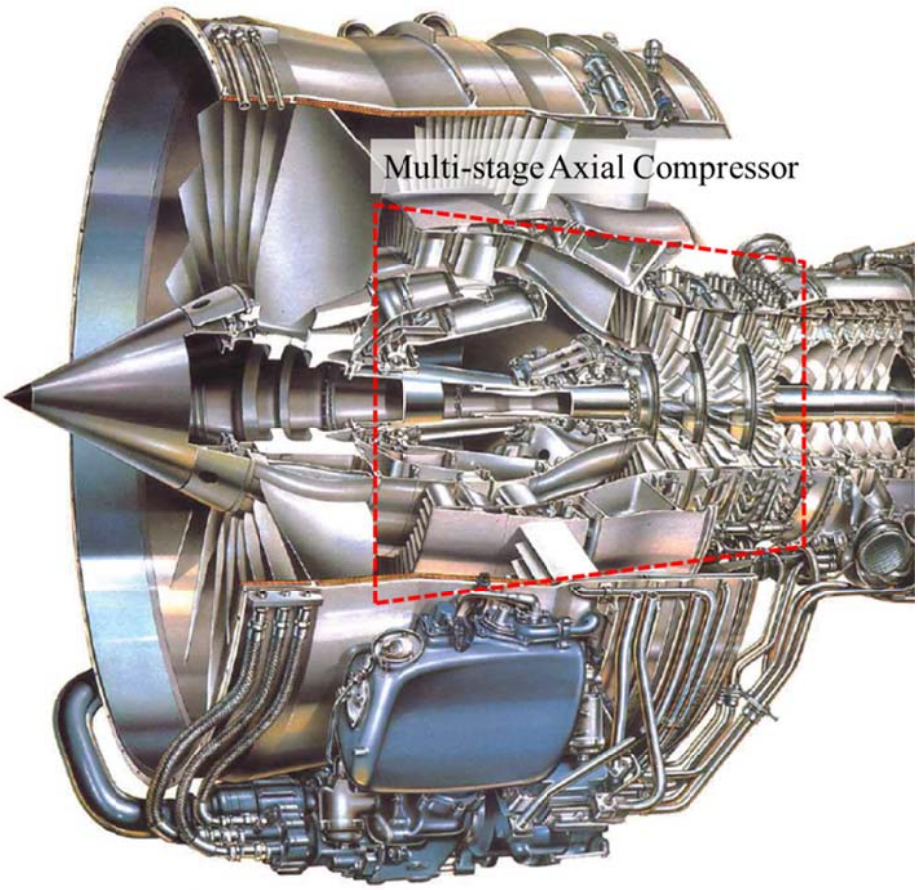

Fig. 1. 1 Illustration of IAE V2500 engine compressor [17]

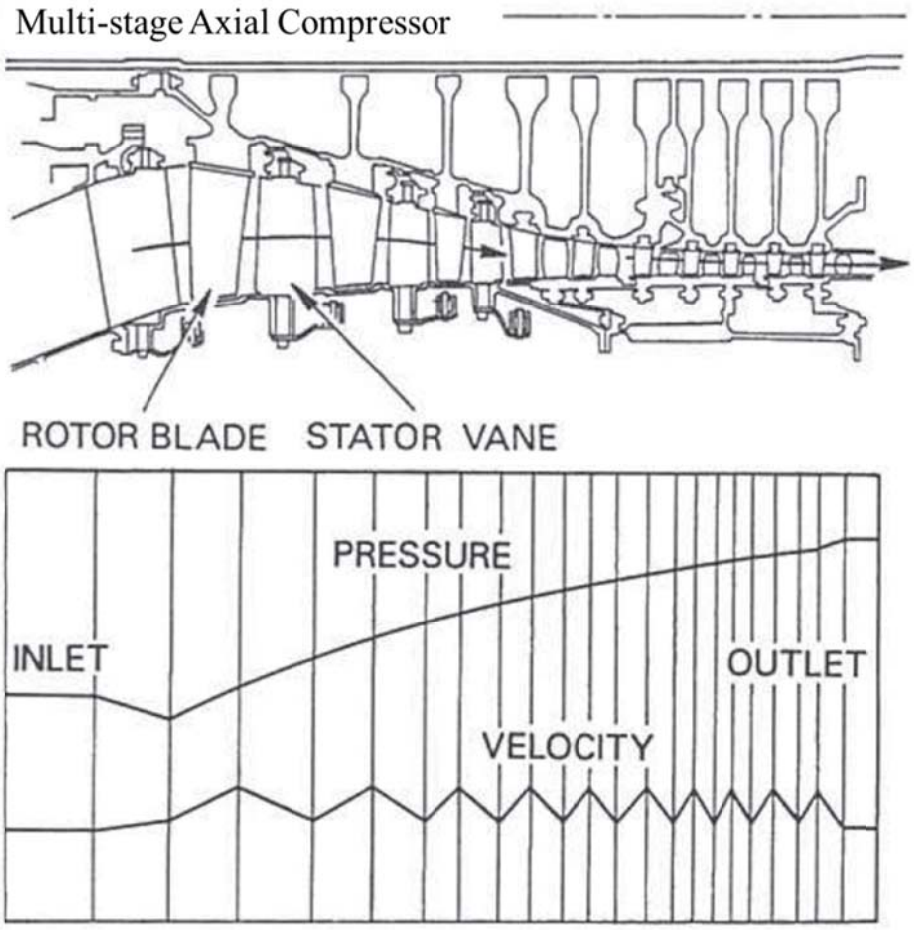

Fig. 1. 2 Cross-section view over a compressor flow path [18]

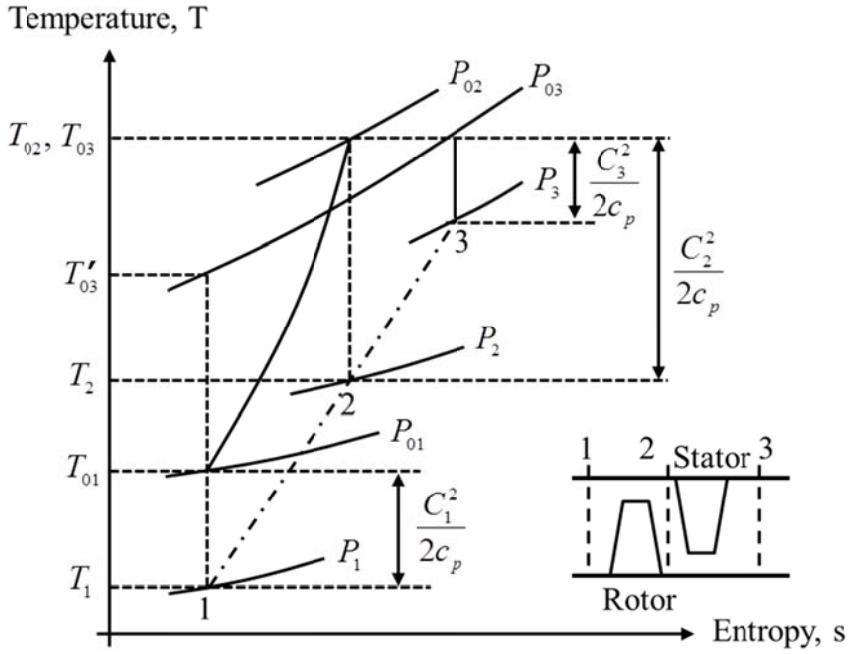

Fig. 1. 3 Compressor stage and T-s diagram [19]

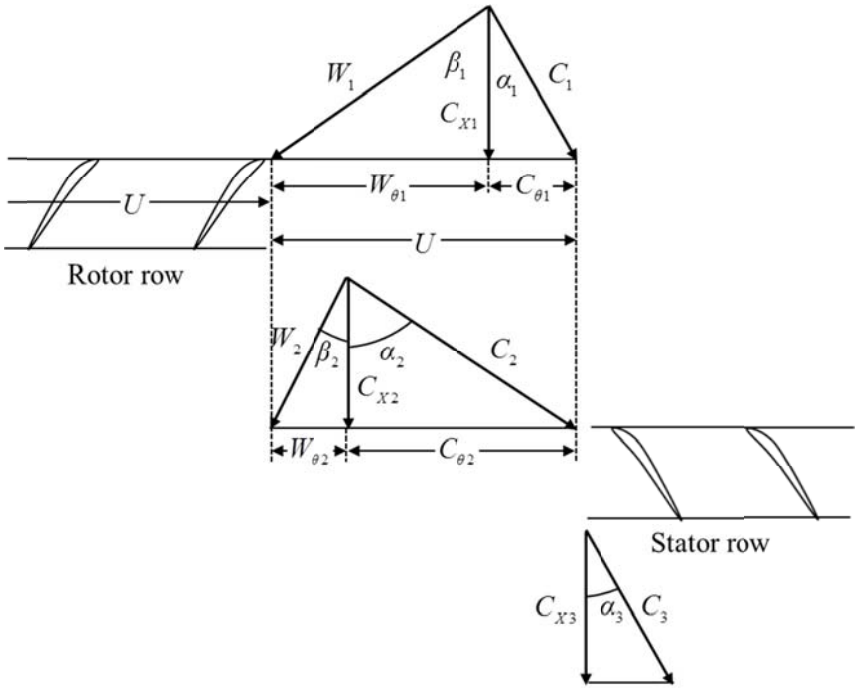

Fig. 1. 4 Velocity triangles for one stage [20]

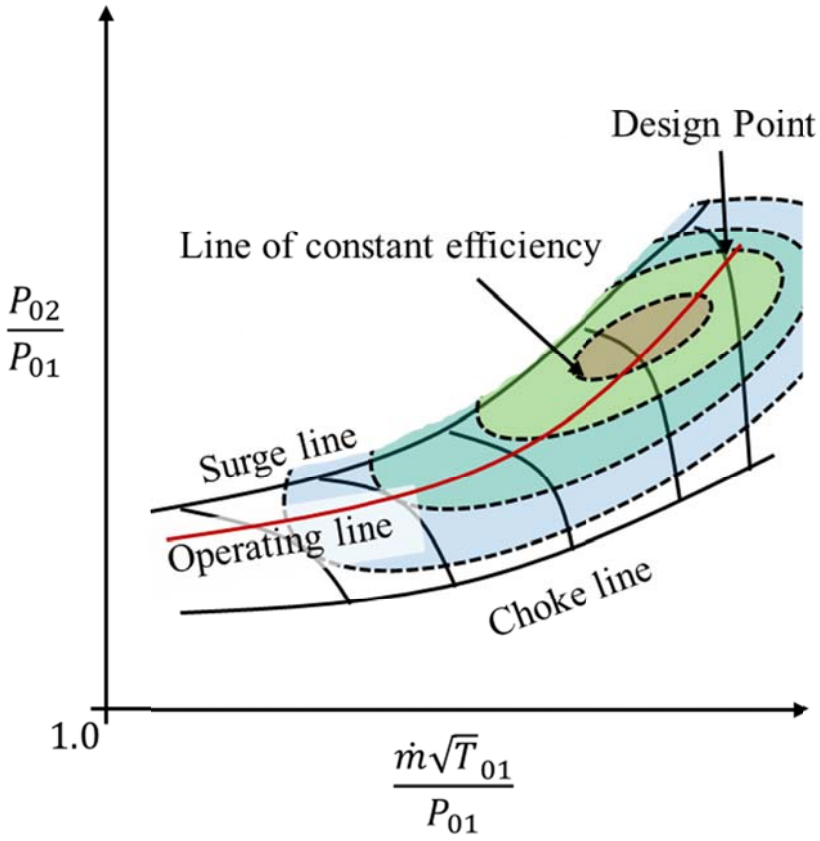

Fig. 1. 5 Schematic illustration of a compressor performance map

Chapter 2. Design Optimization Methods

2.1 Multidisciplinary Design Optimization

The conventional design optimization method usually optimizes each disciplines of the problem separately like Fig. 2.1. This conventional method is easy to apply to design optimization problems since it can use existing analysis tool and optimization method and design optimization process is conducted separately. But it is hard to satisfy every design requirements of each discipline at once, because they are very various and sometimes show opposite tendencies. Therefore, an across-the-board design optimization method for a number of disciplines is necessary to satisfy various requirements of design optimization problem. Multidisciplinary design optimization (MDO) is suggested as one of the representative alternatives for this.

MDO is a branch of design optimization method that uses design optimization technologies to improve design results incorporating a number of disciplines simultaneously as like Fig 2.2. The MDO result of the problem can be superior to the design result by optimizing each discipline sequentially, because it is possible to exploit interactions between the disciplines. But because of interactions and couplings of disciplines, it is not an easy task to predict the behavior of multidisciplinary system accurately, and what is worse is that it requires tremendous analysis time and computing power. Since, if it includes all disciplines of the problem simultaneously, it significantly increases the complexity of the problem. In addition, numerous multidisciplinary analyses are needed during the iterative design optimization process. Hence, efficient design method is the core focus of MDO, and

approximation model has been commonly adapted to a solution of the efficient method in MDO problems.

2.1.1 Framework of MDO and Double-step MDO

A typical MDO process is shown in Fig. 2.3 (a). This process requires a considerable amount of computational time to acquire the aerodynamic performance. For this reason, most optimization cases use the approximation model to reduce the calculation time. However, using the approximation model makes a problem with the accuracy of the solution. To resolve this problem, a double-step MDO process is suggested [23] In Fig. 2.3 (b), the double-step MDO process is presented. In the first step, the optimization process uses an approximation model to find a global optimum with evolutionary algorithm. This optimum point is directly coupled with a CFD/FEA analysis to find the actual global optimum with less error in the second step.

2.1.2 Design Variables and Design of Experiment Analysis

For the baseline rotor shape, multiple curvature arc (MCA) blade is adopted. Design Variables in this study is defined as Fig. 2.4 [24]. The compressor rotor blade is separated into 5 sections along spanwise direction. And each section has 12 design variables.

Design of experiments (DOE) or experimental design is generally the design by information-gathering exercises in the design space that is the region where design variables exist [3, 15, 25-27]. It is needed data about the design space of compressor design optimization which could reproduce the given whole design space to organize the approximate model by DOE. To acquire the accurate data about the given design space for DOE, it is necessary to gain the results of the object function with the optimized

distribution of design variables in the design space. Full factorial design is one of the primary methods of DOE that extracts a large number of experiment points to reproduce the real design space as accurately as possible. In this study, 12 design variables have been selected in 60 design variables by the sensitivity analysis. Thus, if the full factorial design is adapted in the design optimization with 12 design variables, the number of experiment point which is needed to construct DOE is 2^{12} by the 2k full factorial design or 3^{12} by the 3k full factorial design. It is hard to acquire all points of these methods. Therefore, the D-Optimal design is applied to construct the response surface for design optimization efficiently with a lesser number of experiment points. (Fig. 2.5)

The D-Optimal design is the most widely used DOE method by which the experiment points for DOE are selected to maximize a dispersion of a distance between the experiment points in the design space, |XTX| [27, 28]. |XTX| is the determinant of the information matrix (XTX) of the design. This is expected to build an approximate model that could minimize an uncertainty of the undetermined coefficients which is deduced in surrogate model. According to the D-Optimal deign, more than $(n+1)\cdot(n+2)/2$ experiment points are required to construct the approximation model with n design variables. For example, it is necessary more than 21 experiment points with 5 design variables and this is more efficient than the 2k full factorial design with 32 experiment points or the 3k full factorial method with 243 experiment points. For this reason, the D-Optimal design is adopted in this study for screening design space efficiently.

2.1.3 Approximation Model

In this research, Artificial neural network (ANN) and kriging method is used for construction of approximation model. In chatper 3, ANN model is adopted in the first optimization step, kriging model is selected for surrogate model in chapter 4.

ANN model was created based on the ideas of how human nervous system transfers and handles the information. It understands the behaviors of output variables by input variables and defines the relationship between the input variables and the output variables in mathematical form. ANN has a good advantage in representing the nonlinear problems of the complex system [29-31]. In the ANN method, data processing unit which is called 'Artificial Neuron' assemble and judge from the existing state of things in the design optimization problem. Artificial Neuron adds external stimuli with multiplying weighting factors, then deliveries the data to the next neuron by a transfer function. The set of the neurons, which uses same previous data, is defined as 'layer' and the whole artificial neural network is constructed by assembly of the layers. Generally, 3-layer artificial neural network is commonly used and comprised of 'input layer', 'hidden layer', and 'output layer' as like Fig. 2.6. And the mathematical form of this concept is defined like to Eq. (2.1) [31]:

$$a = f\left(\sum_{i=1}^{i=R} \omega_i P_i + b_1\right) \tag{2.1}$$

where a is a vector of output and Pi is a vector of input. And f is the

transfer function, R is the number of input variables, ω_i is the weighting factor and b_1 is a bias vector in Eq. (2.1).

In the case of 3-layer artificial neural network, the input data of input layer is transferred to the output layer through the hidden layer and it draws the output data from the neurons at output layer. The number of neurons at input layer and output layer are same with the number of input variables and output variables. But the relationships between the number of neurons at hidden layer and the number of input variables or output variables are not clearly defined in this process. If the number of neurons at hidden layer is not enough, the design points cannot be represented properly. On the contrary to this, the design points can be represented properly with the large number of neurons at hidden layer. But if the number is too many, the distortion may be occurred in the representation of the other design space by approximation model. Therefore, the proper number of neurons at hidden layer is important factor in the construction of approximation model. As a result of various researches for this problem, it is universally applicable that the number of neurons at hidden layer is set as 1.5~2 times number of neurons at input layer to represent the design space properly.

The Kriging method is approximation model using interpolation. That is, it is geostatistical estimator which predicts value at unknown point weighted by neighbor's distance to the unknown point. Unknown value, Z^*, is obtained from the combination of 4 neighbors and 4 weights as shown in Eq. (2. 2).

$$Z^* = \sum_{i=1}^{n} \lambda_i \cdot Z_i \qquad (2.\ 2)$$

where Z_i is known neighbor value, and λ_i is weight of distance between Z_i and unknown point.

Kriging, of DACE modeling, postulates a combination of a polynomial model and departures of the form given by Eq. (2.3) [32-35]:

$$y(x) = f(x) + Z(x) \tag{2. 3}$$

where $y(x)$ is the unknown function of interest, $f(x)$ is a known polynomial function of x, and $Z(x)$ is the realization of a normally distributed Gaussian random process with mean zero, variance σ^2, and non-zero covariance. The $f(x)$ term in Eq. (3.13) is similar to the polynomial model in a response surface and provides a "global model of the design space; in many cases $f(x)$ is simply taken to be a constant term β.

While $f(x)$ globally approximates the design space, $Z(x)$ creates localized deviations so that the Kriging model interpolates the n_s sampled data points. The covariance matrix of $Z(x)$ is given by Eq. (2. 4).

$$Cov[Z(x^i), Z(x^j)] = \sigma^2 \mathbf{R}[R(x^i, x^j)] \tag{2. 4}$$

where **R** is the correlation matrix, and $R(x^i, x^j)$ is the spatial correlation function between any two of the ns sample points x^i and x^j. The Correlation function $R(x^i, x^j)$ is specified by the user as shown in Table 2.1. The Gaussian correlation function in Eq. (2. 5) is employed in this work.

$$R(x^i, x^j) = \sum_{k=1}^{n_v} \exp\left(-\theta_k \left| x_k^i - x_k^j \right|^2 \right) : i \neq j$$
$$= 1 \qquad : i = j \tag{2.5}$$

where $-\theta_k$ is the correlation parameter in Kriging model. This correlation parameter affects the accuracy of the Kriging method. Thus, it is needed to find the optimized correlation parameter generally [36]. In this work, 'mlefinder.f' and 'krigit.f' which are developed by Simpson and Giunta [32], [33] are used. But, to find correlation parameters, the sequential quadratic programing (SQP) [37, 38] is used instead of the simulated annealing (SA) that used by Simpson in his work [33].

Predicted estimates, $y_{predict}$, of the response at untried values of x are given as follows:

$$y_{predict} = \beta + \mathbf{r}^{\mathrm{T}}(x)\mathbf{R}^{-1}(\mathbf{y} - \mathbf{f}\beta) \tag{2.6}$$

where **y** is the column vector which contains the values of the response at each sample point, and **f** is a column vector which is filled with ones when $f(x)$ is taken as a constant. $\mathbf{r}(x)$ is the correlation vector between length n_s between an untried x and the sampled data points $[x^1, x^2, ..., x^{n_s}]$ and is given by Eq. (2.7).

$$\mathbf{r}^{\mathrm{T}}(x) = [R(x, x^1), R(x, x^2), ..., R(x, x^{n_s})]^{\mathrm{T}} \tag{2.7}$$

In Eq. (2.6) β is estimated using Eq. (2.8).

$$\beta = (\mathbf{f}^{\mathrm{T}}\mathbf{R}^{-1}\mathbf{f})\mathbf{f}^{\mathrm{T}}\mathbf{R}^{-1}\mathbf{y} \qquad (2.\ 8)$$

The estimate of the variance, σ^2, of the sample points from the underlying global model is given by Eq. (2.9):

$$\sigma^2 = \frac{(\mathbf{y} - \mathbf{f}\beta)^{\mathrm{T}}\mathbf{R}^{-1}(\mathbf{y} - \mathbf{f}\beta)}{n_s} \qquad (2.9)$$

The maximum likelihood estimates for the θ_k in Eq. (2.5) used to fit the model are found by maximizing Eq. (2.10) over $\theta_k > 0$.

$$\max_{\theta_k > 0} \frac{[n_s \ln(\sigma^2) + \ln(\det \mathbf{R})]}{2} \qquad (2.10)$$

Both σ^2 and $\det \mathbf{R}$ are functions of θ_k. While any values for θ_k create an interpolative model, the best Kriging model is found by solving the *k*-dimensional unconstrained, nonlinear, optimization problem given by Eq. (2.10).

2.2 Analysis Tools

In this study, we use ANSYS CFX to predict the aerodynamic performance of the compressor. ANSYS CFX is used for analyze and predict the aerodynamic characteristics by many researchers [7, 39, 40]. To generate the meshes, ATM optimized topology is used for the rotor and single passages are included in the computational domain. The ATM optimized method automatically computes a default mesh and sets the base mesh dimensions. Each unique mesh dimension has an edge refinement factor that is multiplied by the base mesh dimension and a global size factor to determine the final size of the mesh dimension [41]. The computational domain consists of 100,000 ~ 150,000 nodes for each computation. As boundary conditions, the ambient total pressure, total temperature and flow directions are given at the rotor inlet and averaged static pressure is specified and allowed to vary at the stator outlet. Progressive increase in the static pressure and velocity components are given at each domain as an initial condition. As a turbulence model, K-epsilon (K-ε) turbulence model is chosen. Scalable turbulent wall function is set as the wall treatment.

Structural analyses such as calculation of compressor weight and safety factor are carried out using the most widely used commercial structural mechanics tool ANSYS. ANSYS has been used in various engineering areas [42-43] including the compressor design and analysis [44-46]. ANSYS solutions provide analysis and simulation tools for various engineering design and optimization problems. It can increase productivity of the design process and minimize practical attempt of prototype in less time by making product development less costly and more reliable. ANSYS can cover various analysis types, elements, materials, equation solvers, and coupled physics for

understanding and solving complex design problems. Therefore, the calculation of safety factor at 1st stage rotor and weight of the whole compressor system using 3D geometry file from AxCent are carried out by ANSYS. The material of the rotor blade is Ti6Al4V. It is a sort of titanium alloy and its maximum yield stress is about 950 MPa. CFD analysis takes about 90~120 minutes and FEA takes about 30~40 minutes in each experiment case and optimization results. These results are calculated by Intel® core™ i7-3770 at 3.40 Hz and ddr-3 32GB ram.

Recently, PIDO (Process Integration and Design Optimization) technology is a necessity in order to enhance the value of Virtual Prototype by integration of CAE tools, automation of complex analysis and design procedures, and optimization of product/process designs. PIAnO is developed based on these PIDO technologies by supported iDOT (ERC, KOSEF/MOST) and it is an abbreviation for Process Integration, Automation and Optimization. Especially, PIAnO provides technologies for design optimization procedures such as DOE method, approximation modeling method, etc. and it has been used in a broad spectrum of engineering design problems [47-50]. In this study, PIAnO is adopted to the DOE process in chapter 4.

Table 2. 1 Correlation Functions for the Kriging Model [34]

Correlation Function	Mathematical Form
Exponential	$\prod_{k=1}^{n_{dv}} \exp(-\theta_k \mid d_k \mid)$
Gaussian	$\prod_{k=1}^{n_{dv}} \exp(-\theta_k \mid d_k \mid^2)$
Cubic Spline	$\prod_{k=1}^{n_{dv}} \begin{cases} \{1-6(\theta_k \mid d_k \mid\}^2 + 6(\theta_k \mid d_k \mid)^3 & \theta_k \mid d_k \mid < 1/2) \\ 2(1-\theta_k \mid d_k \mid)^3 & 1/2 \le \theta_k \mid d_k \mid < 1) \\ 0 & \theta_k \mid d_k \mid \ge 1) \end{cases}$
Matern Linear Function	$\prod_{k=1}^{n_{dv}} [(1+\theta_k \mid d_k \mid) \exp(-\theta_k \mid d_k \mid)]$
Matern Cubic Function	$\prod_{k=1}^{n_{dv}} [(1+\theta_k \mid d_k \mid + \frac{\theta_k^{\,2} \mid d_k \mid^2}{3}) \exp(-\theta_k \mid d_k \mid)]$

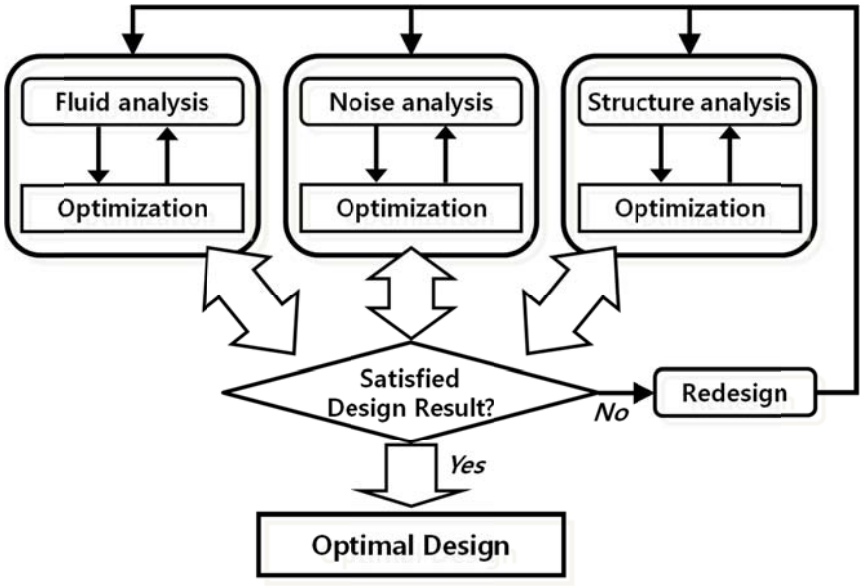

Fig. 2. 1 Conceptual flow chart of conventional design optimization with typical disciplines coupled separately

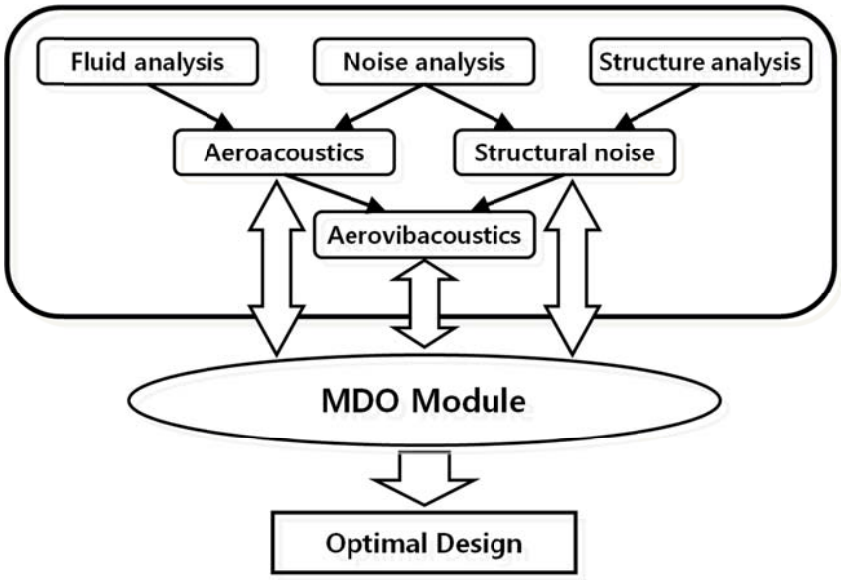

Fig. 2. 2 Conceptual flow chart of design by multidisciplinary design optimization method with various disciplines coupled simultaneously

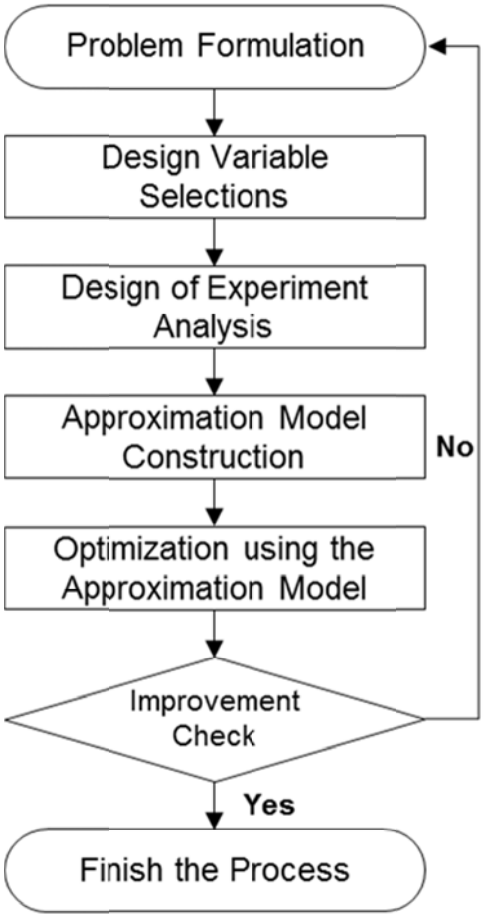
Problem Formulation
Design Variable Selections
Design of Experiment Analysis
Approximation Model Construction
No
Optimization using the Approximation Model
Improvement Check
Yes
Finish the Process

(*a*)

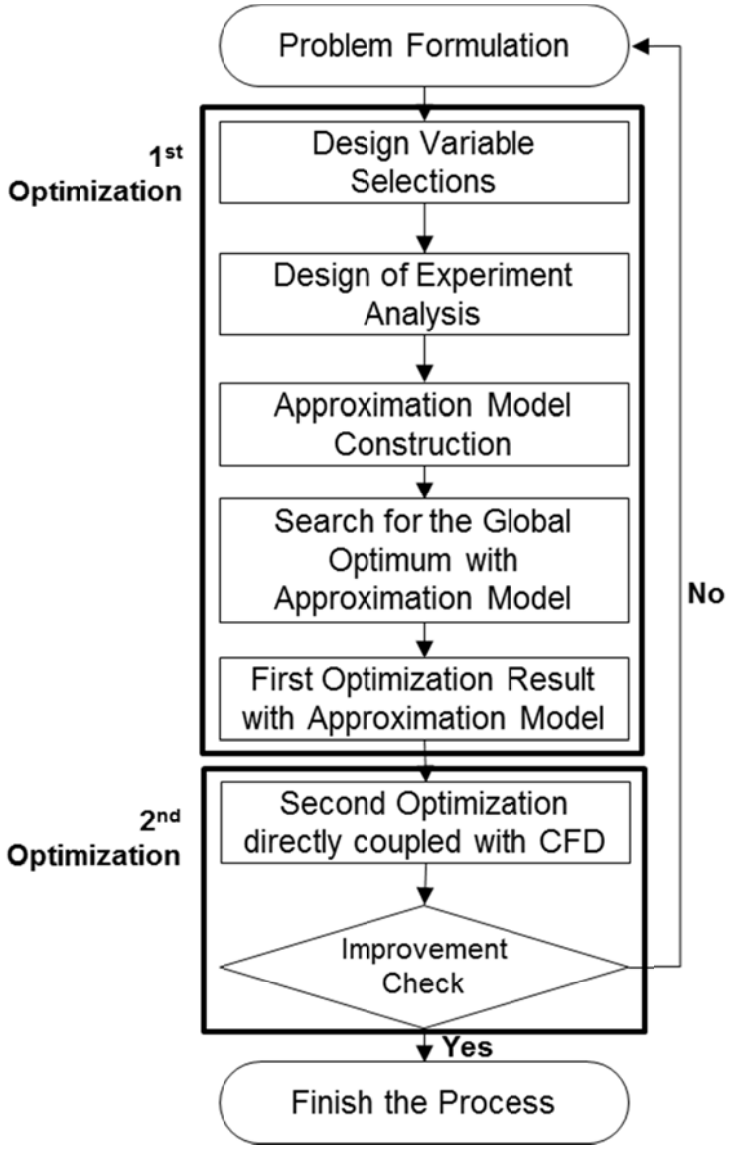

Fig. 2. 3 (a) Flow chart of MDO process based on approximation model and (b) MDO Process with double-steps

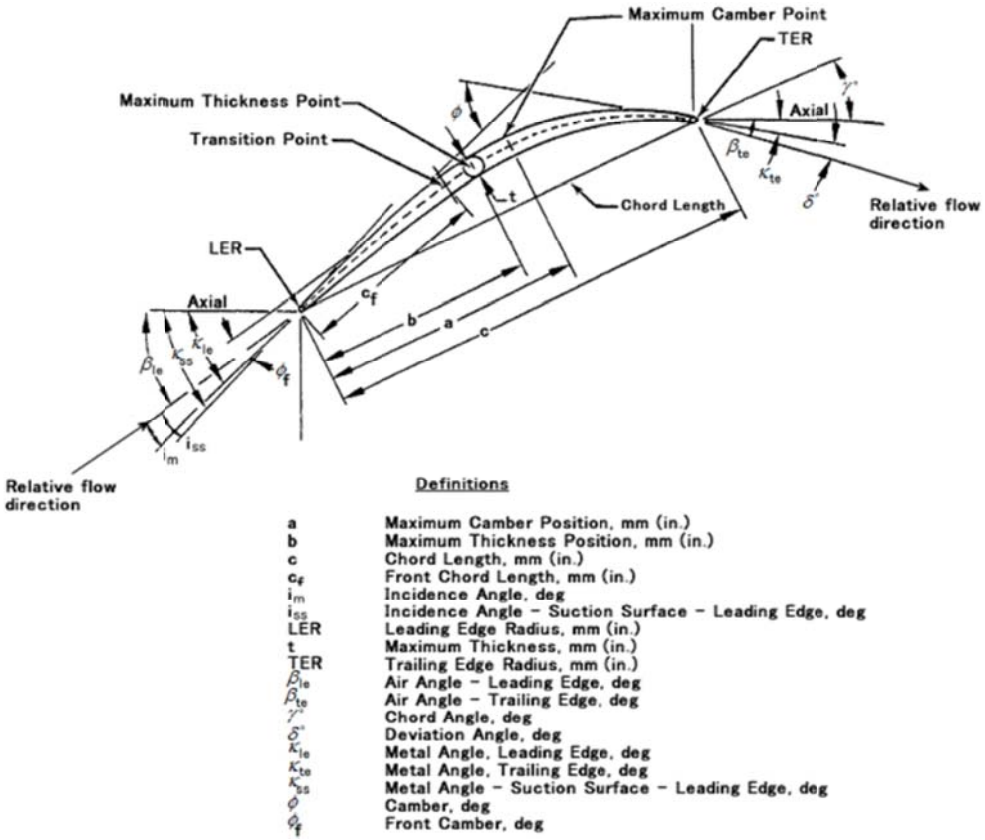

Fig. 2. 4 Design variables of the rotor blade for compressor MDO [24]

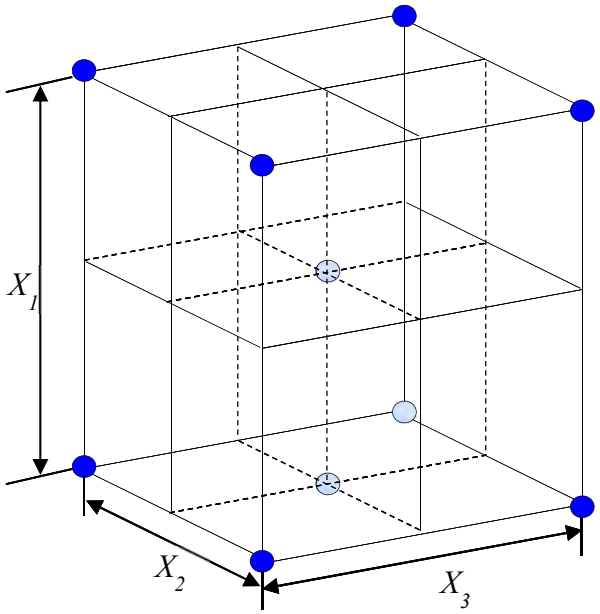

thod

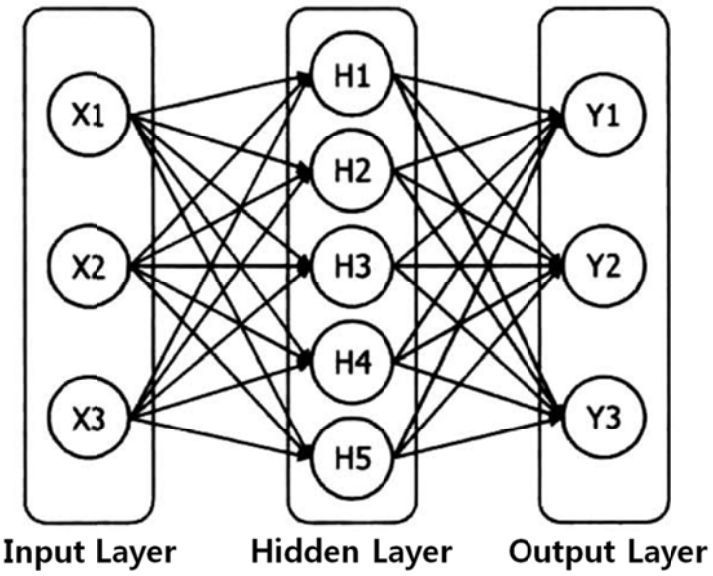

Fig. 2. 6 Concept of 3 layers (Input, Hidden, Output) for Artificial Neural Network approximation model

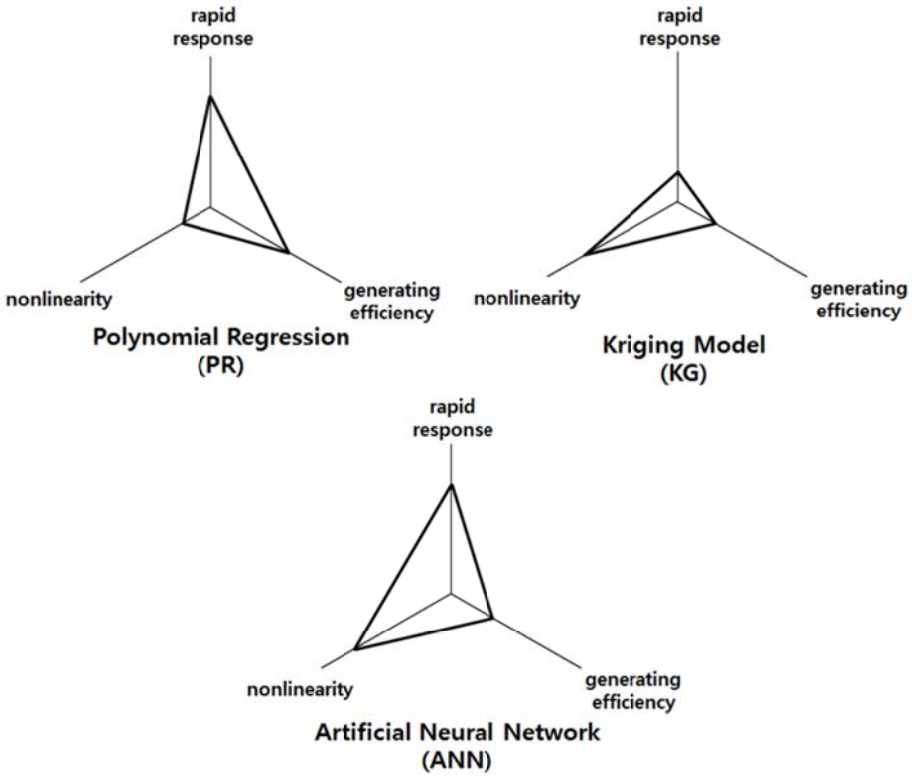

Fig. 2. 7 Comparison of 3 typical approximation modeling methods for the abilities of nonlinearity, rapid response, and generating efficiency

Chapter 3. MDO Framework for Aircraft Axial Low Pressure Compressor at Operating Point

The KARI single-stage low pressure compressor is used as the baseline for the multidisciplinary design optimization (MDO). This compressor is a transonic axial compressor developed by Korea Aerospace Research Institute (KARI) for the engine development program in Korea. The performances and specifications of the baseline and the design target performances are listed in Table 3.1. The design spaces of the KARI low pressure compressor are listed in Table 3.2 and this chapter presents the MDO procedure using these design variables. A flow chart of MDO for the KARI transonic axial compressor is represented in Fig. 3.1. A brief outline of the hybrid MDO procedure is listed as follows:

1. Sample design points based on the selected design variables with the D-optimal method.
2. Evaluate the objectives at the design points with analysis tools of each discipline.
3. Construct an ANN approximation model of the objective function.
4. Perform MDO by Pareto-optimal analysis. (with Approximation model)
5. Perform MDO by Gradient-based method. (without Approximation model)
6. Obtain an optimal compressor design shape.

Compare the objectives of MDO with the results of the initial shape.

3.1 Problem Definition

To construct the objective function for compressor MDO while

considering its aerodynamics and structural performances, the features of each discipline need to be combined. Therefore, the objective function is made up of a multi-objective function that consists of two factors from the aerodynamic and structural disciplines. The factor from the aerodynamic discipline is the adiabatic efficiency (η_{ad}) of the rotor blade that from the structural discipline is the safety factor (SF) of the rotor blade. This multi-objective function is set to maximize the efficiency and the safety factor. It is defined as Eq. (3.1).

$$f = f(\eta_{ad}, SF) \tag{3.1}$$

There are three constraints applied to this problem, and they are listed in Table 2. The safety factor (SF) has to be more than 1.5. It is calculated by the stress of the rotor, which is defined as the ratio of the maximum yield stress (σ_Y) and the calculated maximum stress (σ) as show in Eq. (3.2).

$$SF = \frac{\sigma_Y}{\sigma} \tag{3.2}$$

As in Eq. (3.2), minimization of the stress is equivalent to maximization of the SF.

These multi-objective function and the three constraints are used in the MDO of the given compressor.

$$
\begin{aligned}
&\textit{find} && \textit{Chord length of 3rd, 4th, 5th section, inlet angle of 3rd, 4th, 5th section,} \\
& && \textit{Exit angle of 2nd. 3rd, 4th, 5th section,} \\
&\textit{maximize} && f = f(\eta_{ad}, SF) \\
&\textit{subject to} && \eta \geq \eta_0 \\
& && SF \geq SF_0
\end{aligned}
$$

An aerodynamic analysis is performed using the commercial turbo machinery design tool AxCent™ and analysis tool ANSYS CFX. Structural analyses such as calculation of the weight and the safety factor are carried out using the general commercial tool ANSYS.

3.2 Design of Experiment and Approximation Model

Using an approximation model is reasonable when considering optimization efficiency and the computational costs. For the process of constructing an approximation model, design of experiment (DOE) process is required. DOE is a method of extracting experimental points. There are several types of DOE, such as the 2k full factorial design, the 3k full factorial design, the central composite design, the latin square design and the D-optimal design method. In this study, the D-optimal method was chosen as the D-Optimal method is applied to construct an approximation model effectively as it allows relatively few experiment points. According to the D-Optimal DOE, the experiment points were selected to maximize the range of distances between experiment points in the design space. As mentioned above in chapter 2, more than (12+1)·(12+2)/2 experiment points are required to construct the approximation model with 12 design variables. Minimum experiment points to construct the surrogate model are 91 points. To make

reliable model, in this study, 129 experiment points are selected. From these experimental points, an approximation model was built using an artificial neural network. There are many kinds of approximation model, such as polynomial regression model, the Kriging model [9, 12, 51~54]. An artificial neural network (ANN) method can also be used A polynomial regression model as the response surface model can construct an approximation model efficiently, but it cannot simulate nonlinear characteristics very well. On the other hand, the Kriging and ANN method properly simulate nonlinear characteristics. Consequently, in this case, an approximation model was constructed using an ANN.

3.3 Results and Discussion

An approximation model is built by the D-optimal DOE and ANN methods. The standard type of ANN is selected, with 18 hidden layers. Its transfer function is a sigmoid function, having been trained in this case by experiment points. Generally, the number of hidden layers is nearly 1.5 times the number of variables. In this case, 18 hidden layers are used. The performances of the approximation model are shown in Fig. 3.2 and Fig 3.3. It shows the excellent accuracy of the ANN model. An optimizer is used with a genetic algorithm (GA) for its good ability to find the global optimum [13]. Its population size is 100, and 1000 generations are run. The GA results and Pareto front of the optimization result are shown in Fig. 3.4. The red circles in Fig. 3.4 denote the Pareto front values and filled circles in black are the initial seeds. The empty black circles represent the intermediate points. The structural objective is much more sensitive than the aerodynamic objective in this Fig.3.4. In this study, the design target of safety factor is greater than 2. All domains in this Pareto front chosen satisfy this minimum value.

Consequently, the chosen solution is that with the highest aerodynamic efficiency. The Aerodynamic efficiency (η) of the optimum value increases by 6.23% from the initial value and the structural safety factor (SF) increases by 224.4% in approximation results. The 1st step optimization results are shown in Table 3.3. The results of approximation model have error between surrogate model results and numerical analysis results on the efficiency by 0.42% and the safety factor by 8.32%. It is slight error and quite good fitted results. However, in this research, the increase of objectives is not sufficient to underestimate the error. Therefore, the second step optimization process is utilized. In the second step, the optimizer uses a gradient-based algorithm of the type used for nonlinear continuous optimizations. It starts at the global optimum value to find the accurate result. In this method, the final optimization result is obtained. During 2nd step optimization, derivatives from approximation model are used to examine of direction and step size. The evaluation of objective function is done by numerical analysis at each step. The 2nd step optimization is converged in 4 steps of searching (takes about 6.5 hours). The Isentropic efficiency (η) of an optimum has been improved by 3.69% and the structural safety factor (SF) has been improved by 234.4% compared to those of the baseline model. The shapes of the baseline and final optimized rotor/stage airfoils are shown in Fig. 3.5 and Fig. 3.6. The optimum rotor appears as a gourd bottle. As a result of the prediction, the tip section chord length is increased and thus to take more loading. The inlet and exit angles are also increased. This is quite a good solution for the compressor, but design variables such as C_1, C_3, β_{23}, C_4, β_{14} and β_{15} reach the upper or lower boundary limits. Owing to the limitations of manufacturing device, the design space should be fixed. Table 3 presents the results of the first step and second step optimization. The results of the first step optimization are obtained using

ANN model. In this reason, the results have an error with computation results. This error is solved by gradient-based method in the second step optimization. To search the optimum point, every searching step in gradient-based method performed aerodynamic numerical analysis.

Fig. 3.7 and Fig. 3.8 compare the static pressure distributions at 20% and 80% of the blade span of the baseline and optimized rotors, respectively. The baseline rotor has almost zero incidence angle at blade spans of both 20% and 80%. On the other hand, the optimized rotor shows a relatively large incidence angle near the hub and a zero incidence angle at 80% of the span. This indicates that the optimized rotor distributes more blade loading near the hub and less burden near the blade tip. As the blade tip experiences a high relative Mach number and shock loss, reduced blade loading and pressure gradient alleviate shock losses near the blade tip. On the other hand, as there is some degree of weak shock occurring near the blade hub, the optimized design allows the high blade loading near leading edge of the hub to compensate for reduced blade loading near the trailing edge of the blade.

There is a low momentum fluid region behind the shock wave, which is also a major source of the total pressure loss, thus affecting compression efficiency in a transonic compressor. In the optimized rotor, reduced blade loading near the trailing edge suppresses the flow separation behind the maximum blade thickness location of the compressor, which increases the efficiency the compressor. In addition, the blade tip loading distributions show that there is a steep increase at the pressure side of the optimized rotor. In the optimized rotor, blade shock discontinuities move upstream and are coincident with the blade leading edge. This leads to higher blade loading near the blade tip compared to that of the baseline rotor, ensuring sufficient blade loading at the blade tip. In fig. 3.9, velocity vector of optimum points

flows more smoothly. Entropy of initial point increased at the pressure side trailing edge due to flow separation. In this reason, initial point has a lower efficiency than optimum point.

Fig. 3.11 shows stator velocity vector distributions of the baseline and optimized designs near the hubs. The stator design is largely dependent on the rotor exit flow condition, as the stator inlet angle is matched to the absolute flow angle of the rotor outlet. For this reason, the optimized design reflects the upstream boundary layer effect well and shows near zero incidence. At the same time, there is a flow recirculation region near the hub and shroud of the baseline stator design. The minimized incidence losses in the optimized design also lead to an improvement of the efficiency of the compressor stage.

To verify the safety factor of the rotor, we performed a static structural analysis with ANSYS software. The large values of equivalent Von-Mises stresses were concentrated at the leading edge hub in the baseline model, whereas in the optimized design, the length of the first section (hub section) chord is longer than that of the second section chord. For this reason, the meridional shape becomes a trapezoid, and it drastically relaxes the maximum stresses at the leading edge of the hub. Fig. 3.12 shows a comparison of equivalent stress distributions of the rotor blade. The safety factor increases from 1.3 to 2.9 after the design optimization process.

Given these CFD and FEA results, we concluded that the application of the MDO framework for the compressor design is a suitable means of improving the compressor performance and structural stability of a given design; it is even is applicable to a compressor design that is designed from scratch.

Fig. 3.13 and 3.14 shows the shape of the baseline and optimization results at each step. In these figure, change of the shape is explored along the

optimization process.

For the confirmation of the MDO design capability, we have carried out an actual compressor test to evaluate the aerodynamic performance of the compressor. From the compressor test, we could measure the aerodynamic performance of the compressor at the design point and off-design points to build compressor performance maps based on the test data. Fig. 3.15 and 3.16 shows an overview of the compressor test facility.

Fig. 3.17 shows the total-to-total pressure ratio against the corrected mass flow rate. The star symbols belong to the results of the optimized design of the compressor. The target pressure ratio 1.6 was obtained at a mass flow rate of 15.5 kg/s, which indicates within 1% difference compared to the optimized design. However, the mass flow rate deviates from the design value and begins to reduce before sudden compressor stall occurs. The stall margin in this experiment is defined as follows Eq. (3.3):

$$SM = 1 \quad \frac{\pi_D}{\pi_S}\frac{\dot{m}_S}{\dot{m}_D} \tag{3.3}$$

In this case, stall margin was not considered in the objective function of the MDO framework. As the MDO framework only considers the design point performances, it is necessary to employ features to predict the aerodynamic performances at off-design or near unstable operating points to secure sufficient stall margin at the design process of the compressor.

On the other hand, in Fig. 3.18, isentropic efficiency reaches its design target at the design speed. The peak stage efficiency is about 0.87. It is assumed that at that point, the optimum flow incidence occurs at the rotor leading edge. However, with the occurrence of a positive incidence angle at

the rotor inlet, mass flow rate and efficiency start to decrease while pressure ratio moves horizontally.

This experimental results show that this hybrid multidisciplinary design optimization framework can give a reliable aerodynamic compressor performances.

Table 3. 1 Main compressor design targets

	Design Target	Baseline Design
Mass flow rate	15kg/s	15kg/s
Rotational Speed	22,000 rpm	22,000 rpm
Total-to-Total Pressure Ratio	1.6	1.6
Isentropic Efficiency	More than 0.85	0.84
Rotor Safety Factor	More than 2	1.3

Table 3. 2 Selected design variables after sensitivity analysis

Design Variables	Lower Boundary	Baseline	Upper Boundary
Chord, C_1 (X1)	46.05	52.33	58.61
Chord, C_2 (X2)	46.85	53.23	59.62
Inlet angle, β_{12} (X3)	-43.63	-49.58	-55.53
Chord, C_3 (X4)	48.59	55.21	61.84
Exit angle, β_{23} (X5)	-35.43	-40.26	-45.09
Inlet angle, β_{13} (X6)	-50.47	-57.35	-64.23
Chord, C_4 (X7)	49.76	56.54	63.37
Exit angle, β_{24} (X8)	-40.12	-45.59	-51.07
Inlet angle, β_{14} (X9)	-52.3	-59.43	-66.56
Chord, C_5 (X10)	51.28	58.28	65.27
Exit angle, β_{25} (X11)	-47	-53.41	-59.82
Inlet angle, β_{15} (X12)	-54.7	-62.15	-69.61

Table 3. 3 Results of 1st step optimization

Design Variables	Baseline	Optimum	
Chord, C1 (X1)	0.0495	0.0549	
Chord, C2 (X2)	0.0490	0.0505	
Inlet angle, β12 (X3)	-51.0	-47.09	
Chord, C3 (X4)	0.0482	0.0579	
Exit angle, β23 (X5)	-25.0	-40.25	
Inlet angle, β13 (X6)	-52.0	-54.48	
Chord, C4 (X7)	0.0480	0.0537	
Exit angle, β24 (X8)	-32.0	-47.87	
Inlet angle, β14 (X9)	-55.0	-59.43	
Chord, C5 (X10)	0.0470	0.0553	
Exit angle, β25 (X11)	-38.0	-56.08	
Inlet angle, β15 (X12)	-59.0	-62.15	
Efficiency	84.53%	87.17%	86.81%
Safety Factor	2.869	3.324	3.048
		surrogate	numerical

Table 3. 4 Results of 2nd step optimization

Design Variables	Baseline	Optimum
Chord, C1 (X1)	0.0495	0.053
Chord, C2 (X2)	0.0490	0.0554
Inlet angle, β12 (X3)	-51.0	-47.09
Chord, C3 (X4)	0.0482	0.0579
Exit angle, β23 (X5)	-25.0	-41.46
Inlet angle, β13 (X6)	-52.0	-54.48
Chord, C4 (X7)	0.0480	0.0565
Exit angle, β24 (X8)	-32.0	-47.15
Inlet angle, β14 (X9)	-55.0	-58.98
Chord, C5 (X10)	0.0470	0.0611
Exit angle, β25 (X11)	-38.0	-55.91
Inlet angle, β15 (X12)	-59.0	-65.26
Efficiency	84.53%	87.09%
Safety Factor	2.869	3.176

Table 3. 5 Comparison of double-step optimization results

	Aerodynamic Efficiency (%)		Safety Factor	Calculation Time (hrs)
Initial Design	84		1.5	
Double step optimization : 1st step	MDO Design (Approximation model results)	87.17	3.26	18 hrs
	CFD(FEM) Results	86.81	3.05	1hr 20min
	Test Results	85.7	N/A	
Double step optimization : 2nd step	MDO Design (Gradient based method results)	87.1	3.18	6hrs 30min

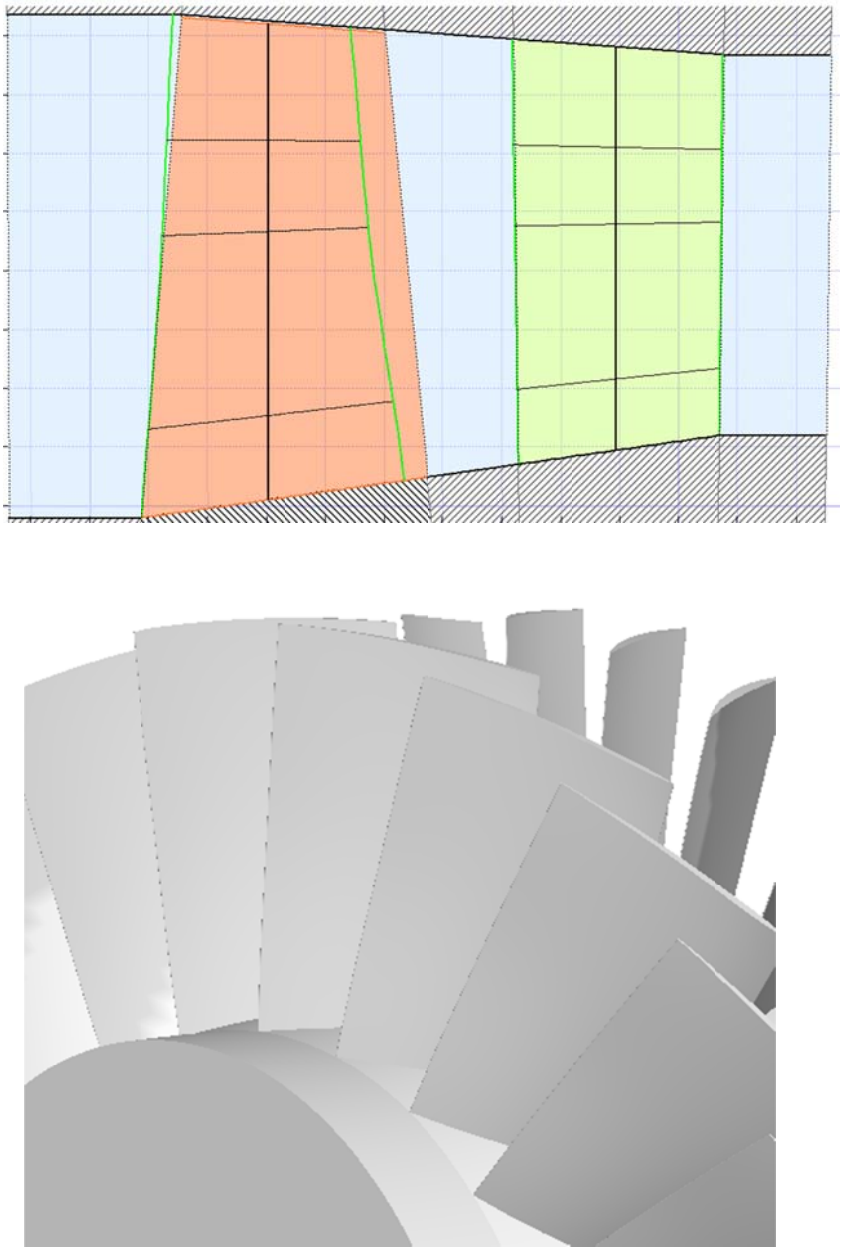

Fig. 3. 1 (a) Meridional view of baseline compressor and (b) 3D shape of baseline compressor

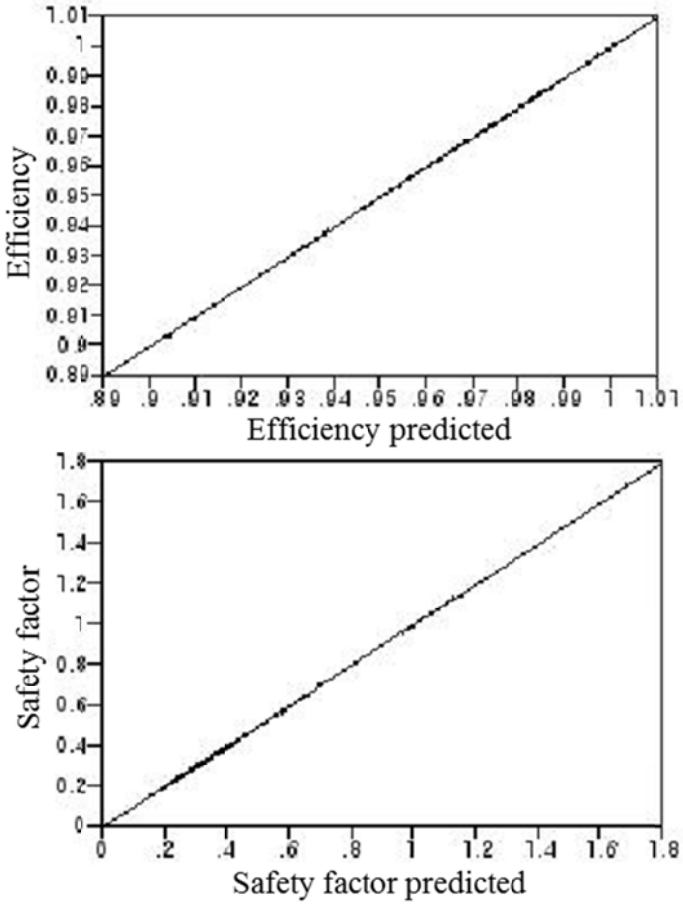

Fig. 3. 2 Actual values versus predictions from approximation model

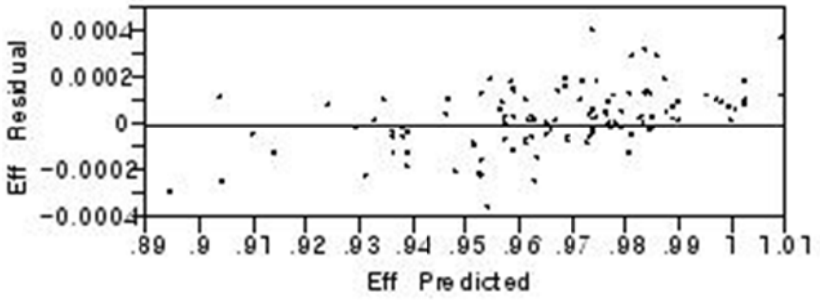
Eff Residual
0.0004
0.0002
0
-0.0002
-0.0004
.89 .9 .91 .92 .93 .94 .95 .96 .97 .98 .99 1 1.01
Eff Predicted

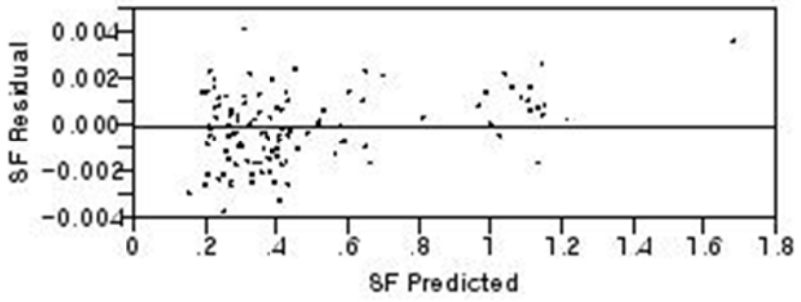
SF Residual
0.004
0.002
0.000
-0.002
-0.004
0 .2 .4 .6 .8 1 1.2 1.4 1.6 1.8
SF Predicted

model

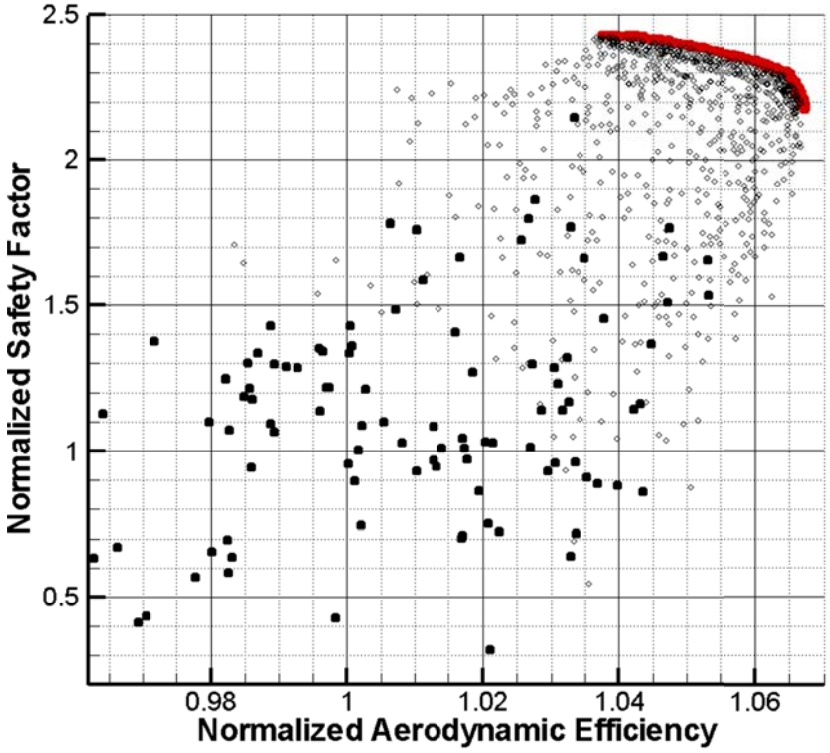

Fig. 3. 4 Pareto Front From First Step Optimization

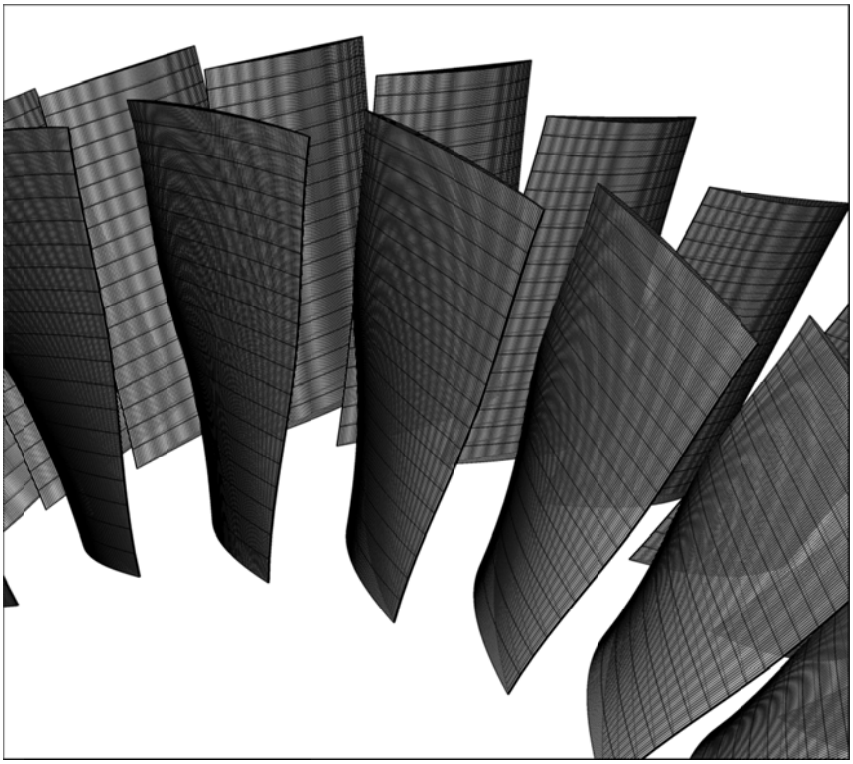

Fig. 3. 5 Baseline compressor rotor/stator rows

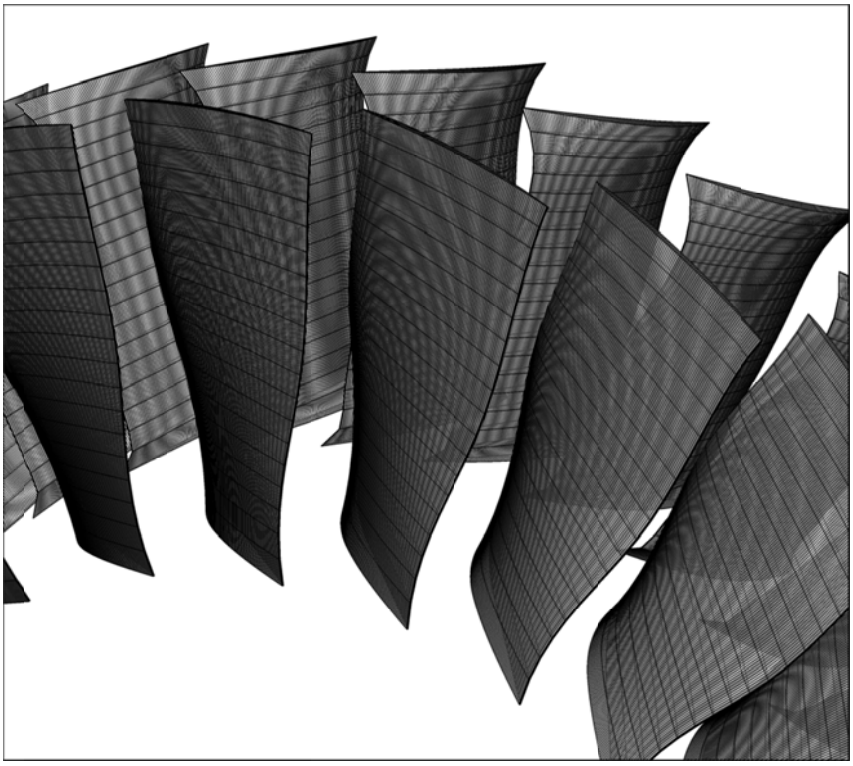

Fig. 3. 6 Optimized compressor rotor/stator rows

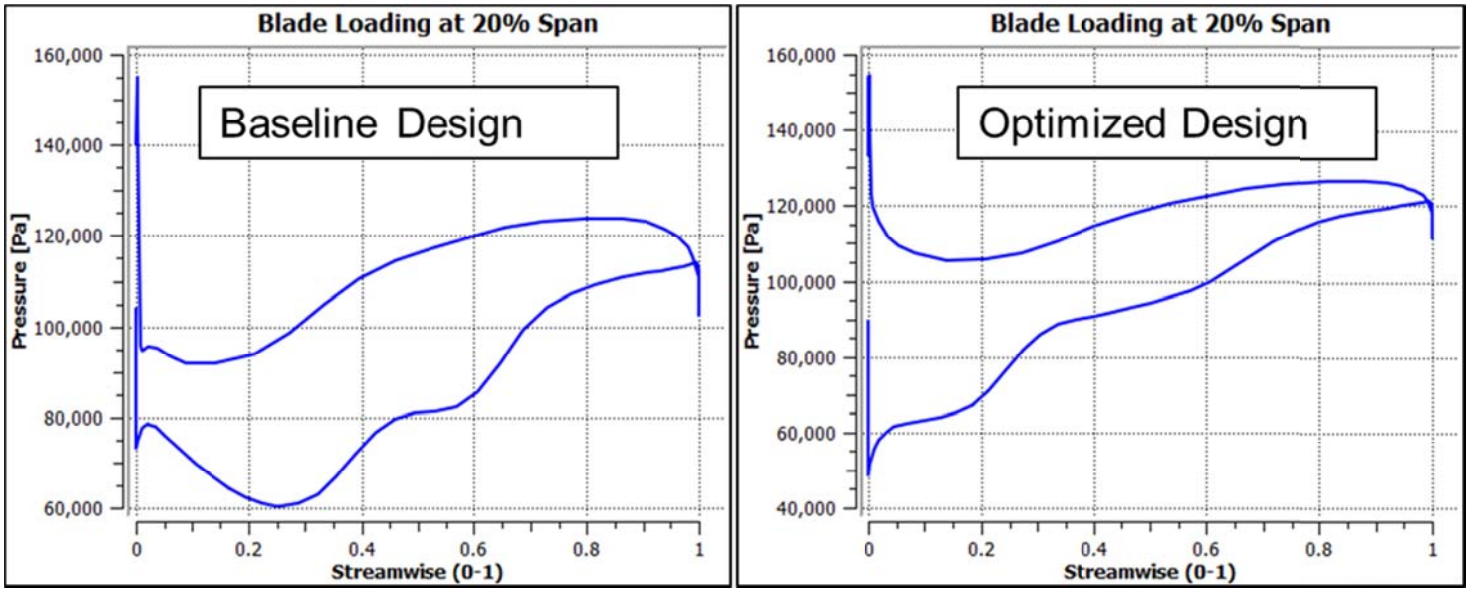

Fig. 3. 7 Static pressure distributions at 20% span of the blade

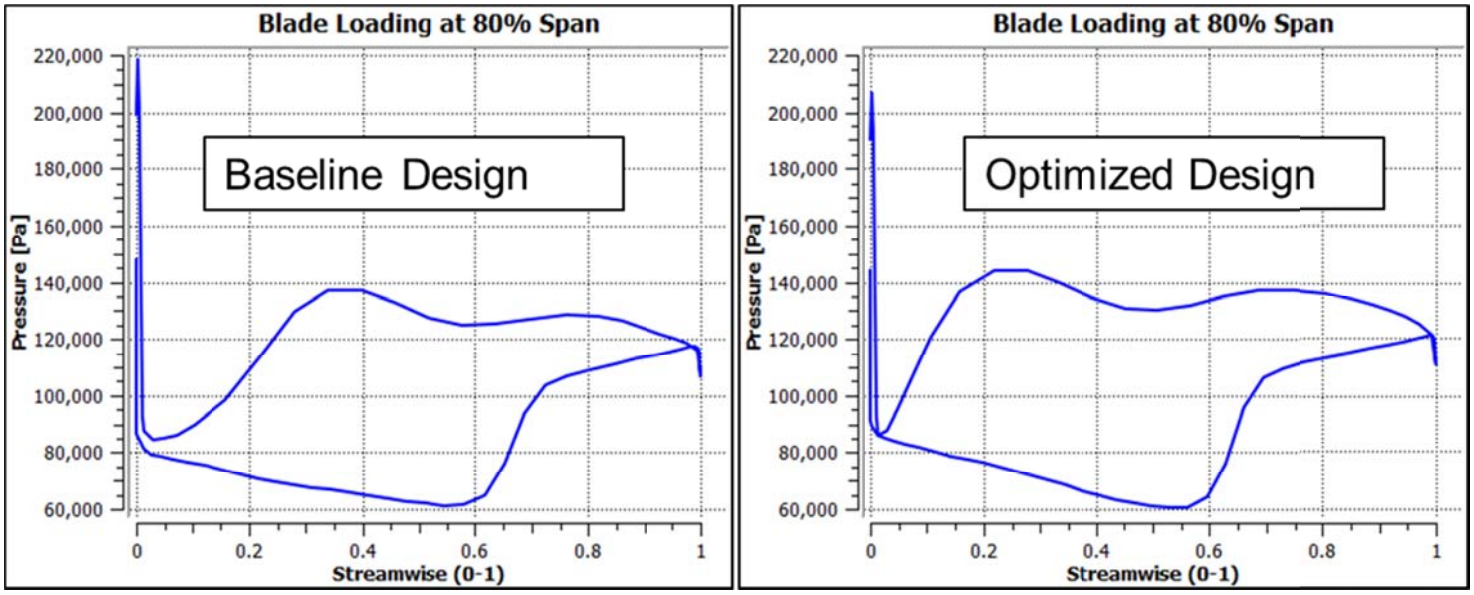

Fig. 3. 8 Static pressure distributions at 80% span of the blade

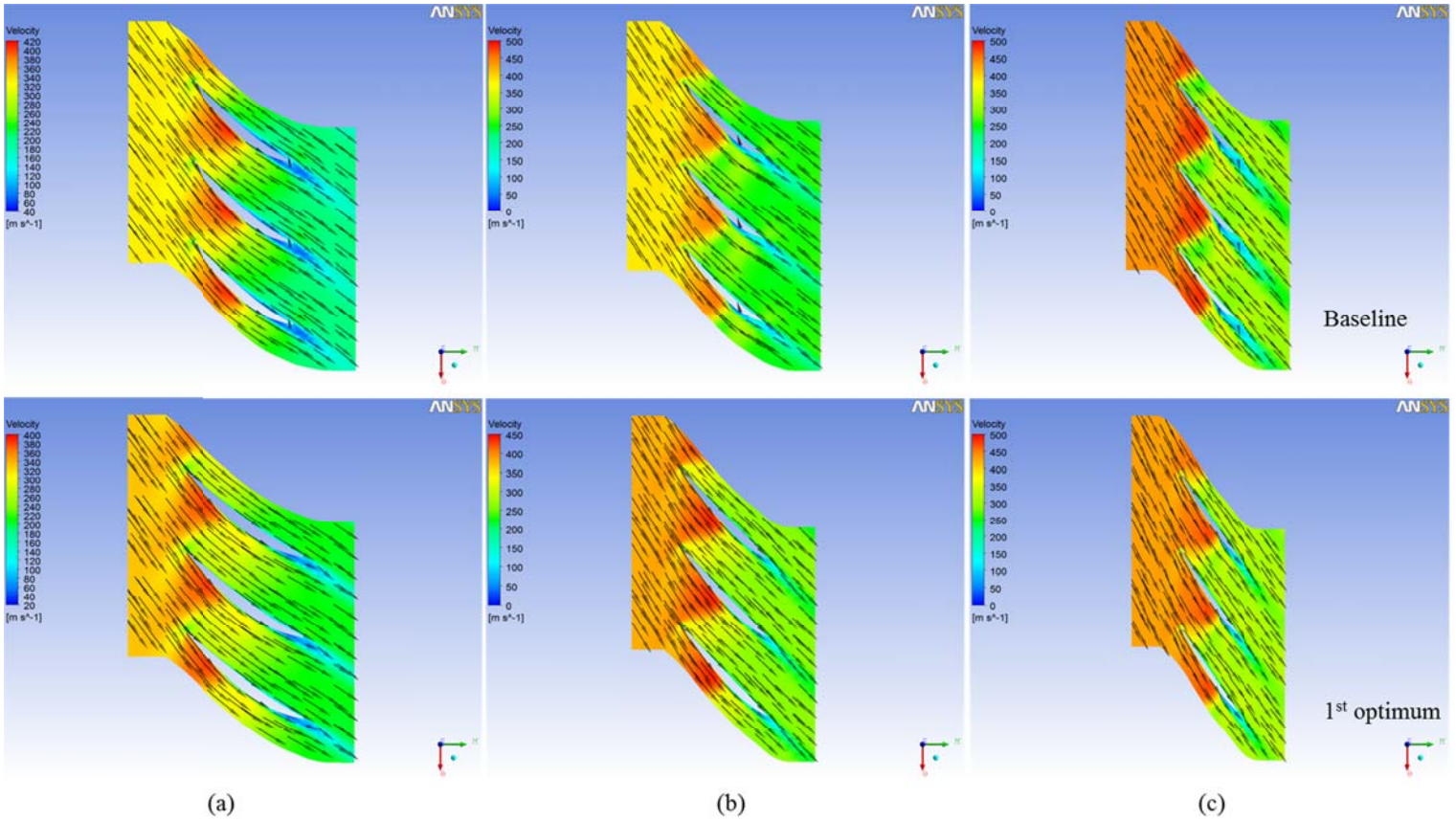

Fig. 3. 9 Mach number contour with velocity vector at (a) 20%, (b) 50%, (c) 80% span

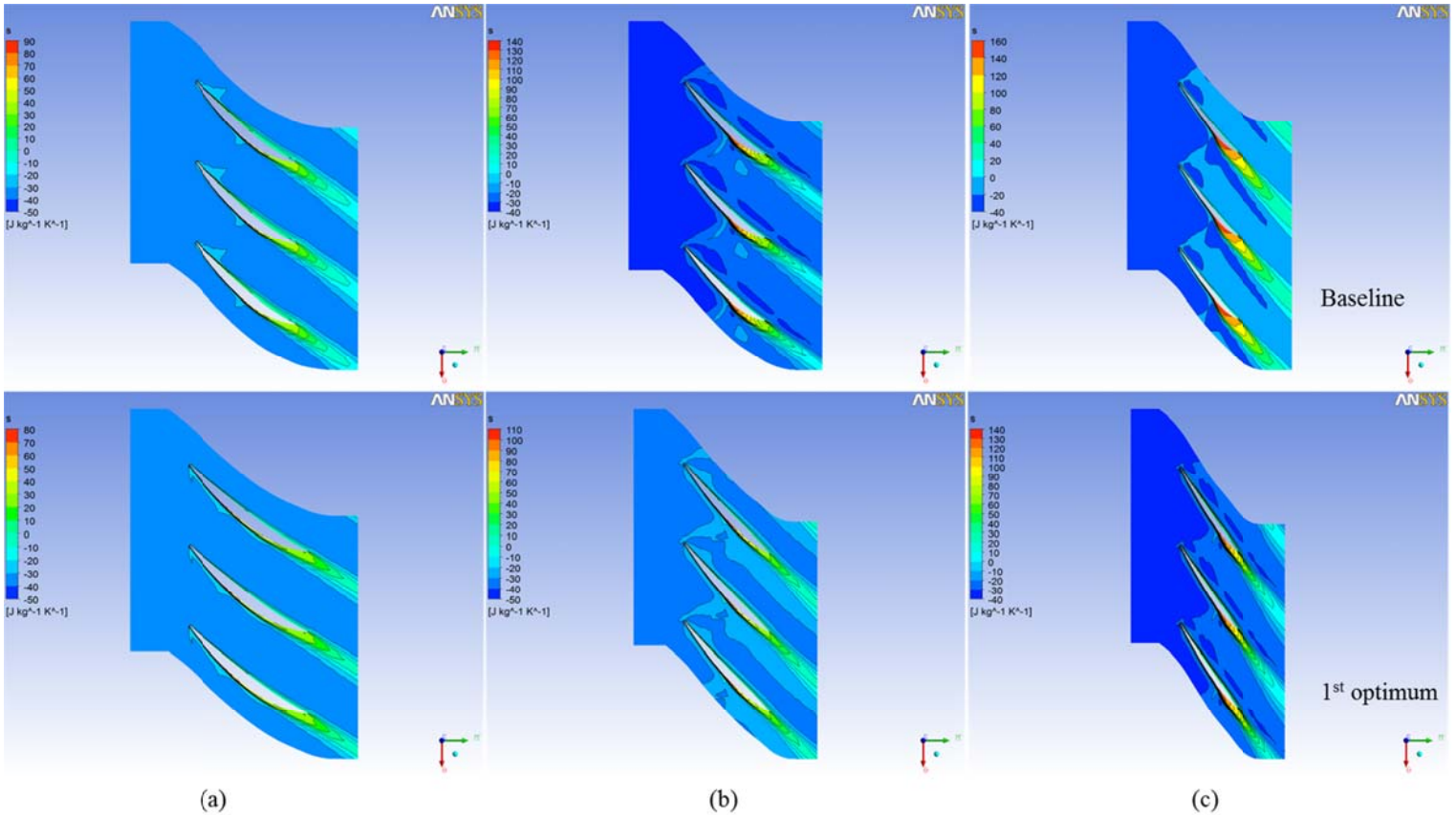

Fig. 3. 10 Entropy contour at (a) 20%, (b) 50%, (c) 80% span

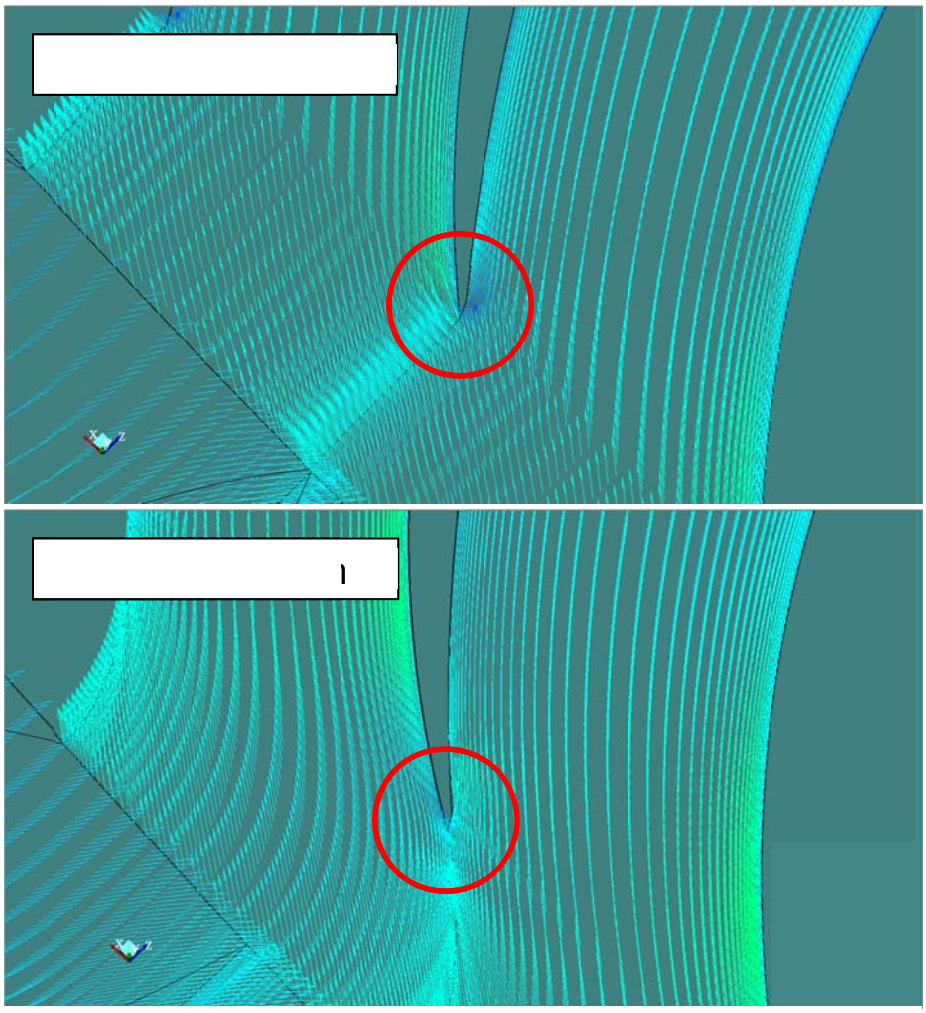

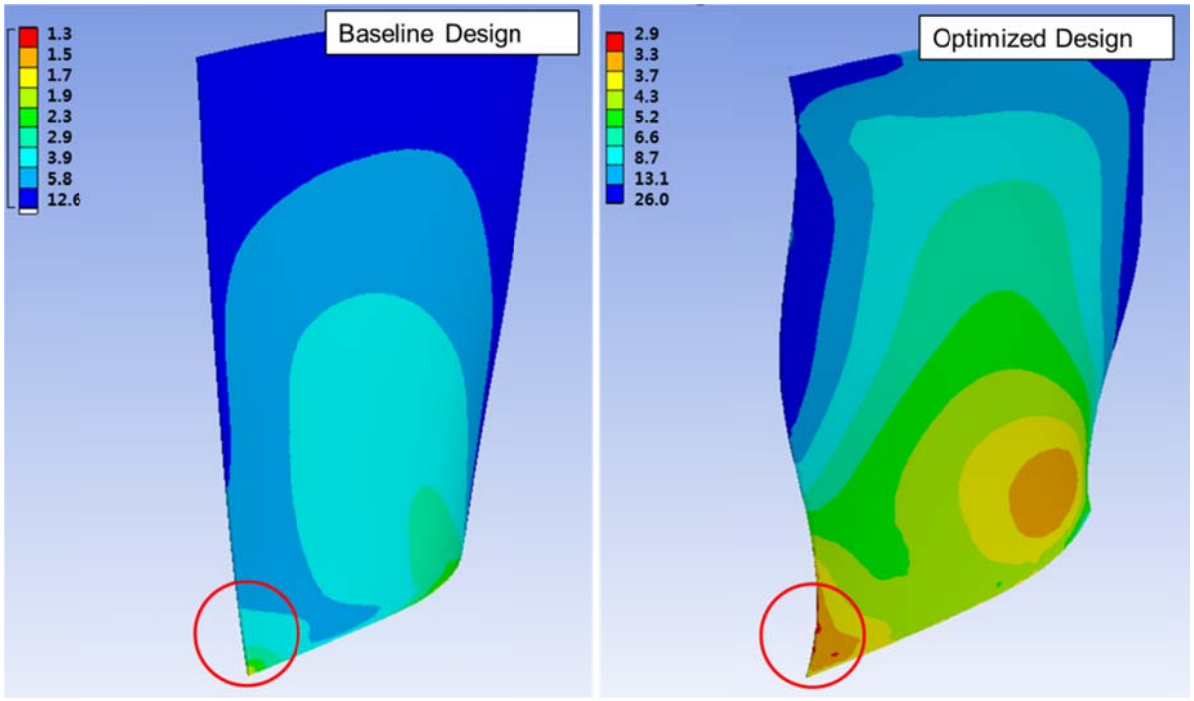

Fig. 3. 12 Equivalent Stress Distributions in Rotor Blades

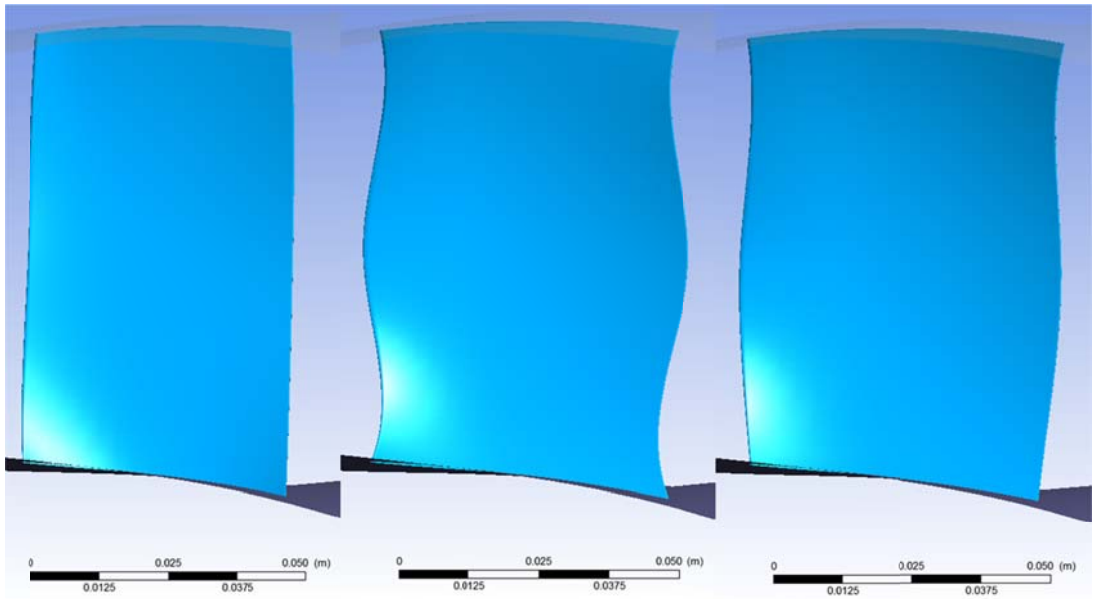

(a) Initial shape (b) 1st step result (c) 2nd step result

Fig. 3. 13 Shape of the optimization results

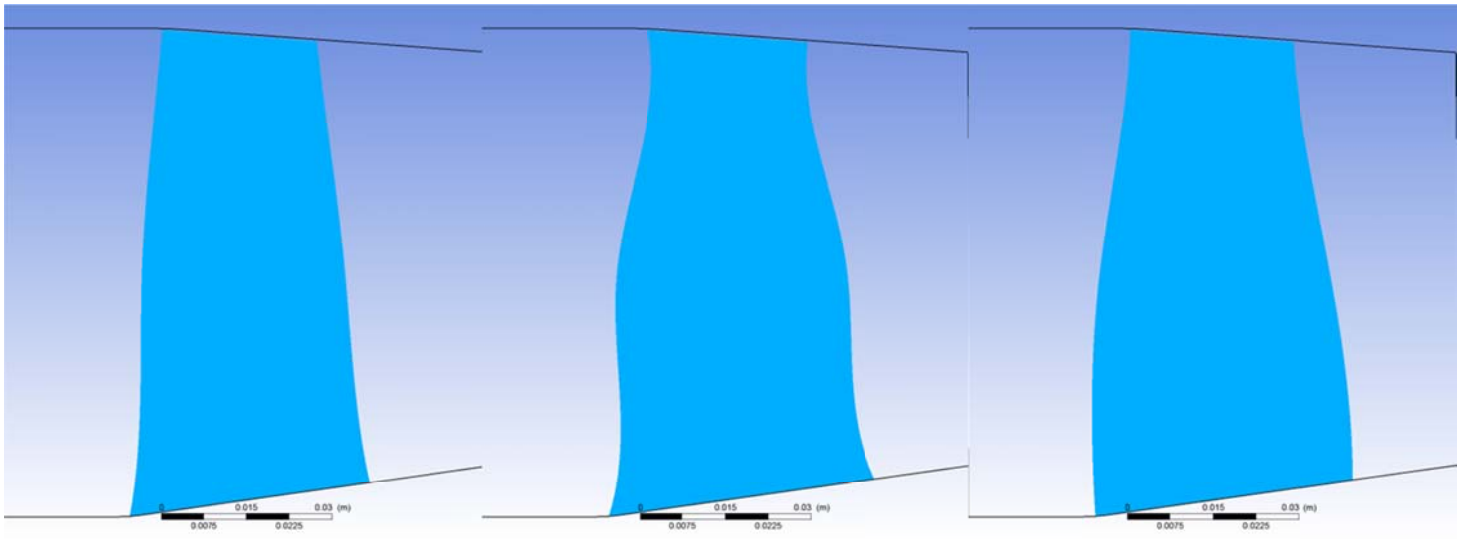

(a) Initial shape (b) 1st step result (c) 2nd step result

Fig. 3. 14 Meridional view of optimization results

Fig. 3. 15 Front view of the test section [55]

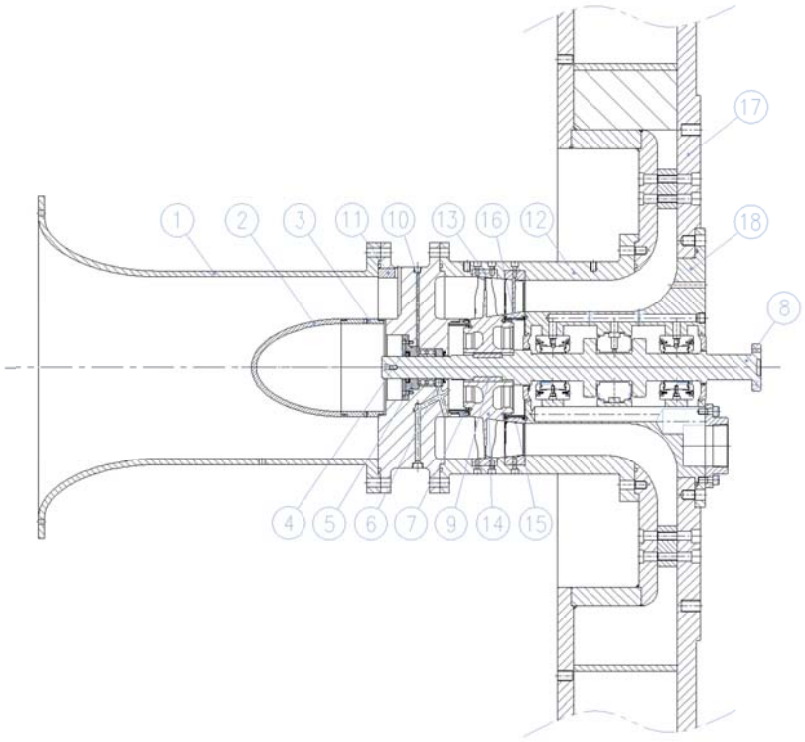

Fig. 3. 16 Meridional view of test apparatus [55]

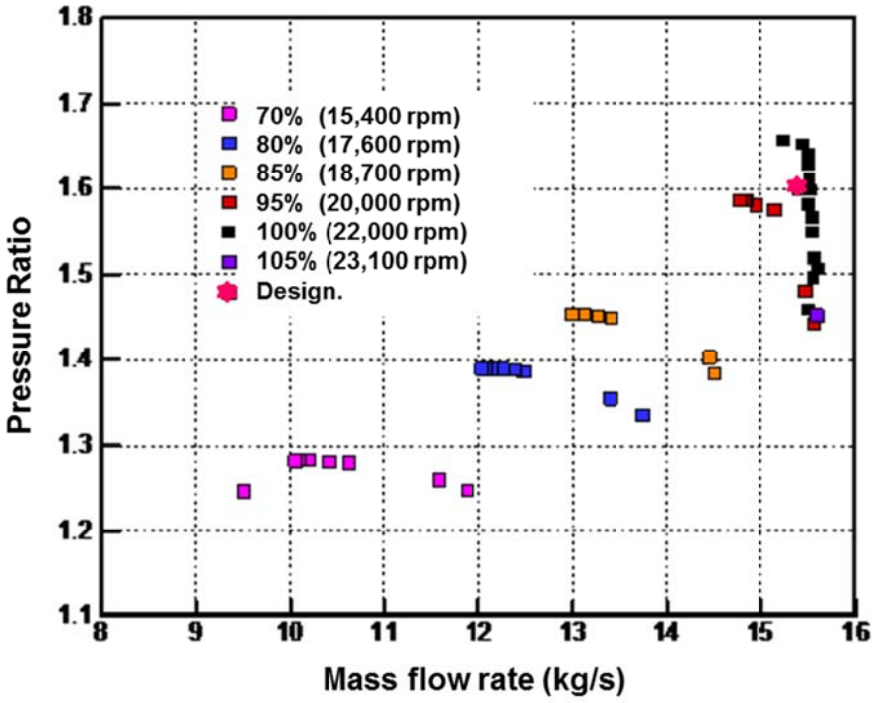

Fig. 3. 17 Total-to-total pressure ratio of the optimized compressor stage [55]

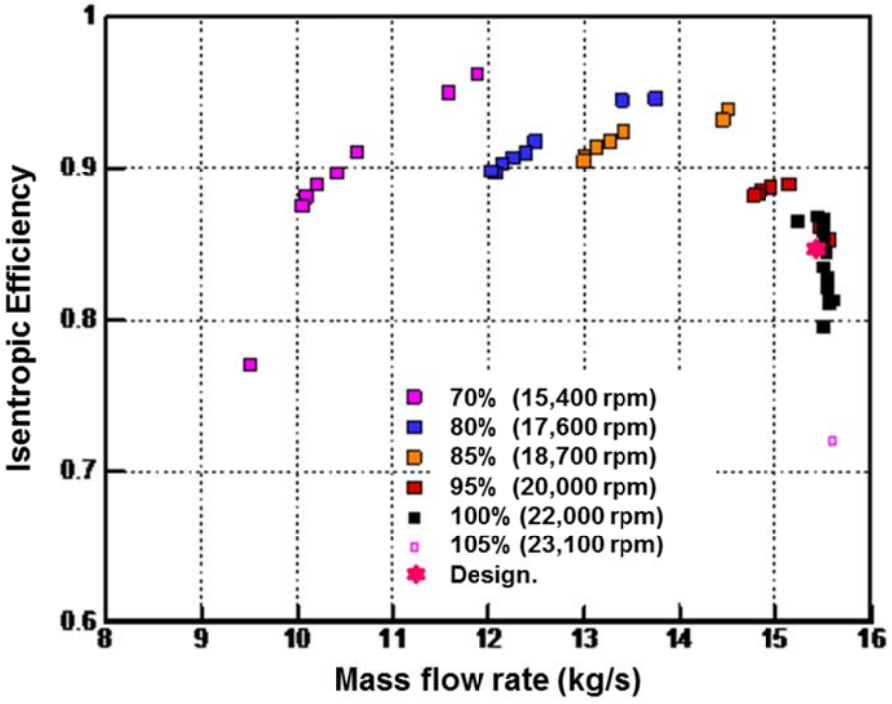

Fig. 3. 18 Isentropic efficiency of the optimized compressor stage [55]

Chapter 4. MDO Framework for Aircraft Axial Low Pressure Compressor with Securing Operating Margin

4.1 Problem Definition

To construct the objective function for compressor MDO while considering its efficiency and stable operating condition, the features of each discipline need to be combined. Therefore, the objective function is made up of a multi-objective function. The adiabatic efficiency (η) of the rotor stage, the Lieblein diffusion factor (DF), and the safety factor (SF) are objectives in this study. This multi-objective function is set to maximize the efficiency and minimize the diffusion factor. It is defined as Eq. (4.1).

$$f = f(\eta, \frac{1}{\mathrm{DF}}) \qquad (4.1)$$

Lieblein diffusion factor was originally defined in terms of a correlation between deceleration of the suction surface flow and the wake momentum thickness. It was expressed in terms of cascade area ratio and turning through the blade row. For incompressible flow with equal axial velocity into and out of the cascade,

$$\mathrm{DF} = \left(1 - \frac{\cos\beta_1}{\cos\beta_2}\right) + \frac{\cos\beta_1}{2S}(\tan\beta_1 - \tan\beta_2). \quad (4.2)$$

The Lieblein DF accounts for static pressure rise and flow turning in the blade passage. There are compressor geometries with a DF=0.7 greater than

the “critical value” in which the passages are free of hub-corner stall [8]. And Suder et al. and Khaleghi et al. studied about injection angle effects on the working stability. In that study, the diffusion factors in various injection conditions are compared and it shows that stall occurs when the diffusion factor at tip exceeds a value of about 0.75 [56, 57]. In this study, Lieblein diffusion factor will be used for foresee the stall margin qualitatively. S is the solidity, the ratio of the blade chord length and pitch length. β is a mass averaged flow angle.

The stall margin (SM) can be defined by calculation of the mass flow rate and the pressure ratio at the stall point. SM is defined by Eq. (4.3) [58].

$$SM = \left[\frac{PR_{stall} \times \dot{m}_{ref}}{PR_{ref} \times \dot{m}_{stall}} - 1 \right] \times 100 \qquad (4.3)$$

Design constraints are defined as the objective performance. Equality constraints are mass flow rates and pressure ratio and inequality constraint is the efficiency of baseline compressor.

These multi-objective function and the three constraints are used in the MDO of the given compressor. And design variables are defined as like chapter 3.

$$\begin{aligned} &\textit{find} && \textit{Chord length of 3rd, 4th, 5th section, inlet angle of 3rd, 4th, 5th section,} \\ &&& \textit{Exit angle of 2nd. 3rd, 4th, 5th section,} \\ &\textit{maximize} && f = f(\eta_{ad}, SF, 1/DF) \\ &\textit{subject to} && \eta \geq \eta_0 \\ &&& SF \geq SF_0 \\ &&& DF \leq DF_0 \end{aligned}$$

4.2 Design of Experiment and Approximation Model

In this chapter, the approximate model of kriging method for MDO is formulated by applying experiment points which are extruded by the D-Optimal method. The approximation model of kriging method consists of input with 10 chosen design variables and output with 3 responses (the efficiency, diffusion factor, safety factor). The accuracy of the approximation model can be determined by calculating of the coefficient of determination (R2) and the root mean square error (RMSE). In this study, all values of R2 exceed 0.99; therefore, the approximation model in this work simulates the actual design space well, highlighting its reliable.

Aerodynamic Numerical analysis is done by ANSYS CFX and Structural analysis is done by ANSYS Workbench.

4.3 Results and Discussion

With this MDO process, satisfactory optimum results are obtained. With multi-objective function considering the adiabatic efficiency, the Lieblein diffusion factor, and the safety factor, the efficiency is increased by 4.49% and diffusion factor is decreased by 4.4%, and the safety factor is significantly increased by 13.6%. The shape of optimum result is shown in Fig.4.1.

Fig.4.2 is a pressure contour in blade-to-blade view of baseline rotor. Upper figure is contour at 50% span. In that figure, distinct normal shock wave is located at 60% chord of pressure side and 20% chord of suction side of next rotor blade. Lower figure is that of 98% span. Near the tip section,

flow is in the transonic region. And the shock wave located at 60% chord of pressure side and the inlet of suction side.

Fig. 4.3 shows a pressure contour in blade-to-blade view of optimized rotor. As above, Upper figure is contour at 50% span and lower figure is 98% span. In upper figure, the shock wave located at the leading edge of suction surface and 55% chord of pressure side. And lower figure, 98% span, also shows the shock wave located at leading edge of suction side. It helps the working flow streaming uniformly and decreases the losses.

In Fig. 4.4 at leading edge, optimized rotor flows more smoothly than baseline shape and separation region is slightly narrow. In that reason, the efficiency and the diffusion factor has better performances in the optimum result.

Structural analysis result is shown in Fig. 4.5. Baseline shape has a peak loaded stress at the hub corner of leading edge. With fixed C1 and C2, equivalent stress is much decreased at hub section.

Fig. 4.6 to 4.8, the blade loading at 25%, 50%, 98% span is drawn. At 25% and 98% span length, all blades have a near zero or negative incidence angle to avoid an occurrence of stall. However, at 50% span, the initial rotor has a positive incidence angle and it can cause a separation or a stall. The optimized shape turns the inlet angle to make the zero incidence angle.

Fig. 4.9 shows mach number contour and velocity vectors. At initial point, stronger shock wave is occurs than optimum point and working fluid flows more efficiently in optimum shape. In Fig. 4.10, increase of entropy is bigger in initial point at trailing edge than optimum point. It causes the loss of aerodynamic performances.

Initial and Optimum design variables and performances are in table 4.1. Lengthened chords make the more work in tip section and adjusted inlet, exit

angles move the shock wave position.

With Eq. (4.3), SM is calculated from the baseline working area data and the optimum working area data. The working area data is calculated with increasing the outlet boundary static pressure. From those results, SM of the baseline is 28% and SM of the optimum is 33.6%. It is over-estimated than the experimental result. It is a limit of the numerical analysis predicting the stall point. However, from a qualitative side, the SM is increased by 19.7%.

In Fig. 4.11, the working map of the compressor is presented. The blue dots are the optimum results and the red dots are the baseline results. The points of lower-left side are the design points. The distance between design point and near stall point in blue dots is longer than that of red dots. It can approve the extension of operation area.

Table 4. 1 Design variables and performances of initial and optimum point

Design Variables	Baseline	Optimum	
Chord, (X1)	0.055	0.058	
Chord, (X2)	0.046	0.048	
Inlet angle, (X3)	-45.292	-47.675	
Chord, (X4)	0.052	0.055	
Exit angle, (X5)	-38.417	-40.439	
Inlet angle, (X6)	-51.769	-54.494	
Chord, (X7)	0.051	0.054	
Exit angle, (X8)	-44.703	-47.056	
Inlet angle, (X9)	-54.549	-57.42	
Chord, (X10)	0.057	0.06	
Exit angle, (X11)	-50.579	-53.241	
Inlet angle, (X12)	-57.961	-61.012	
Efficiency	86.84%	87.78%	87.76%
Diffusion Factor	0.526	0.503	0.505
Safety Factor	2.473 (fixed hub)	2.809	2.795
		surrogate	numerical

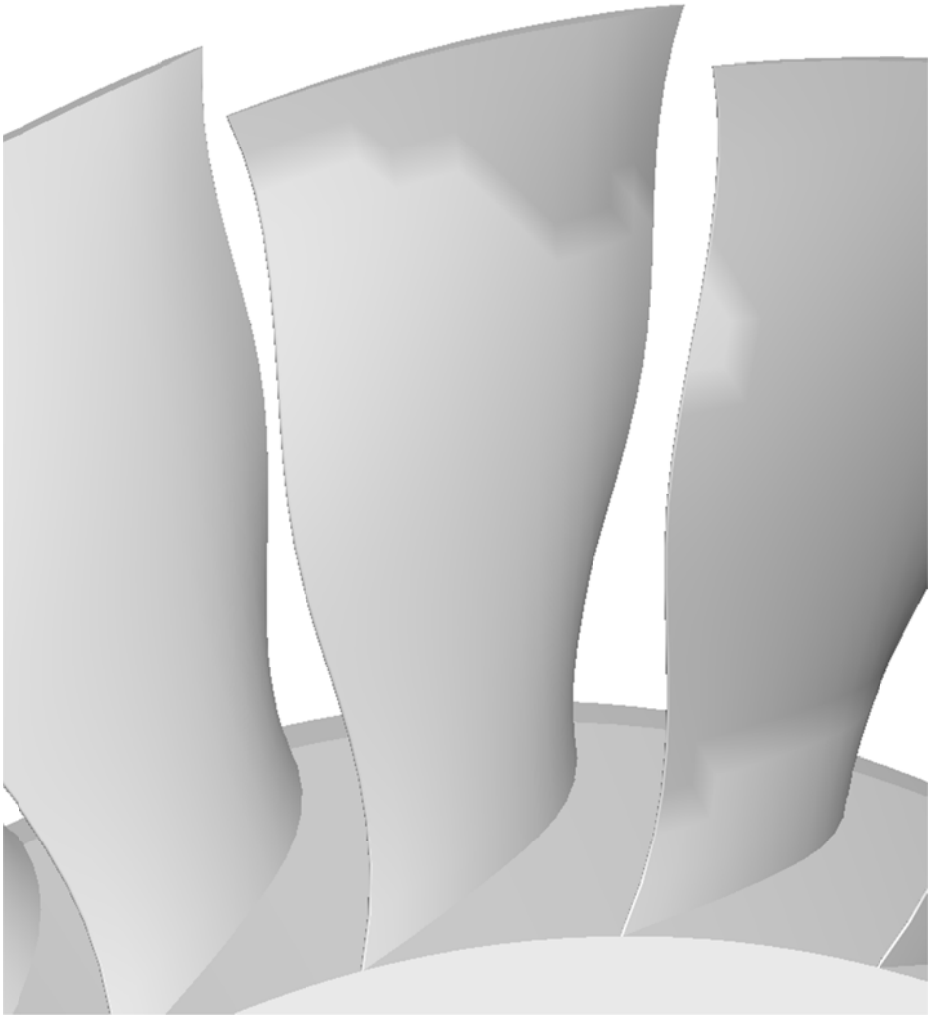

Fig. 4. 1 Shape of optimization result

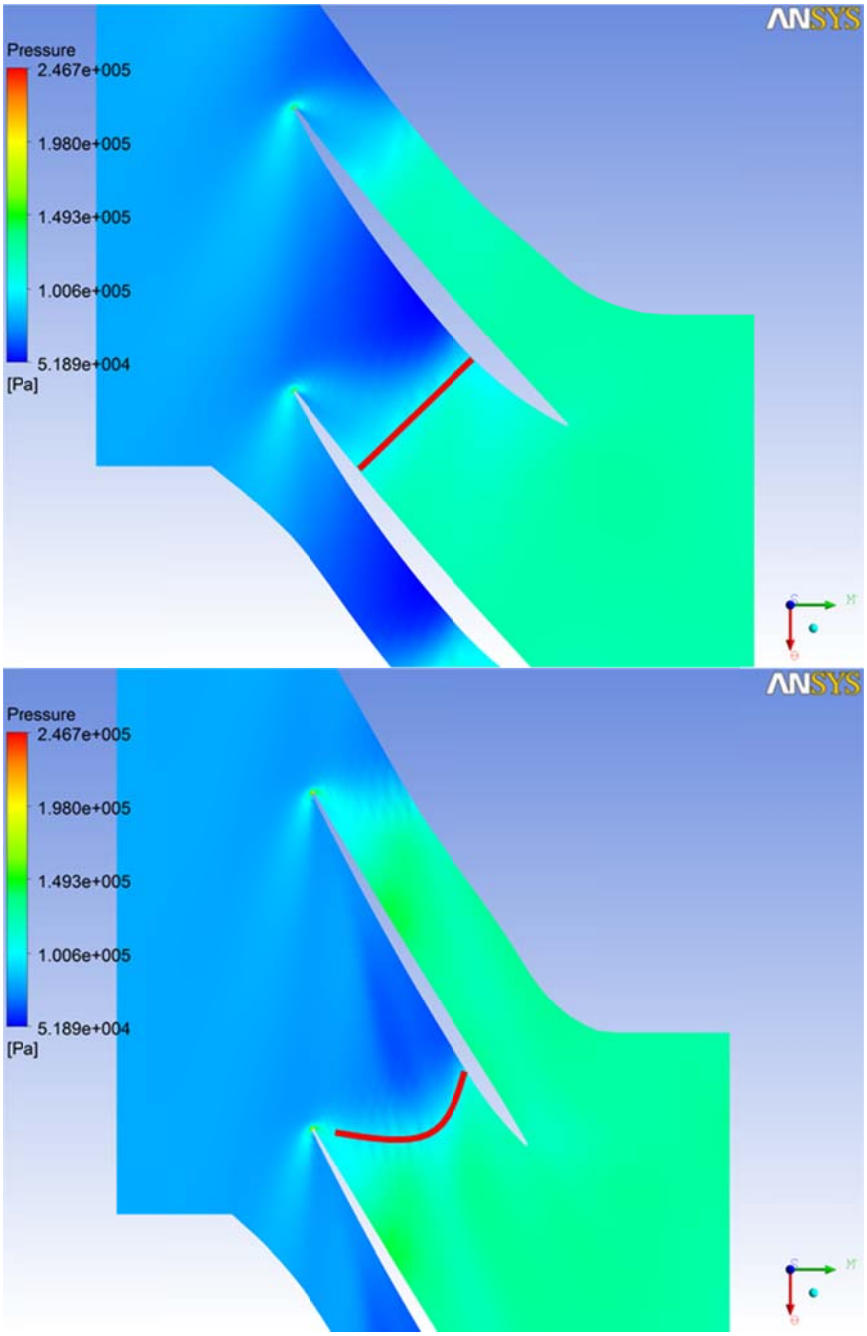

Fig. 4. 2 Pressure contour at 50% span (upper), 98% span (lower) of baseline rotor

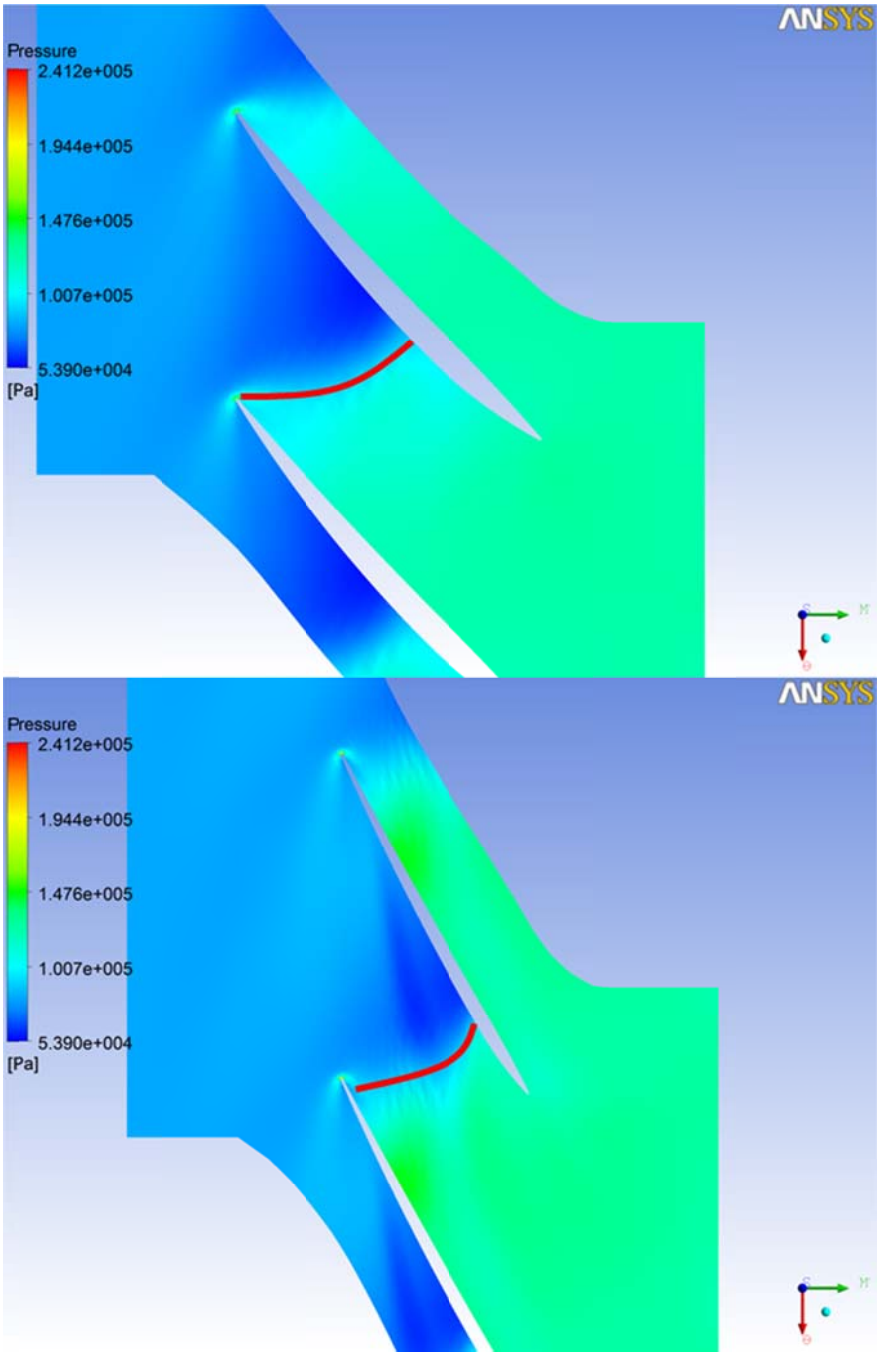

Fig. 4. 3 Pressure contour at 50% span (upper), 98% span (lower) of optimized rotor

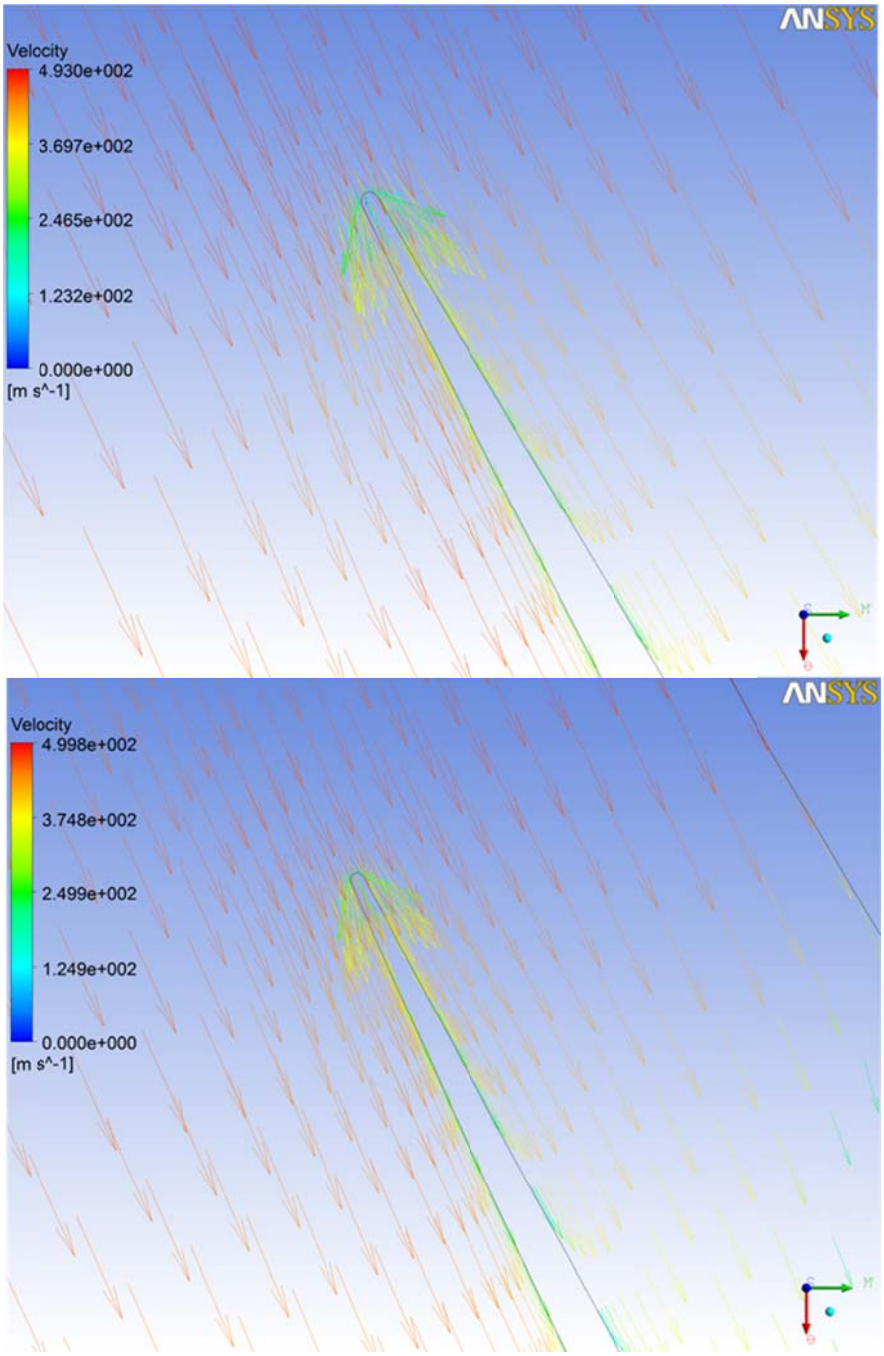

Fig. 4. 4 Velocity vector at 98% span leading edge of baseline (upper) and optimized rotor (lower)

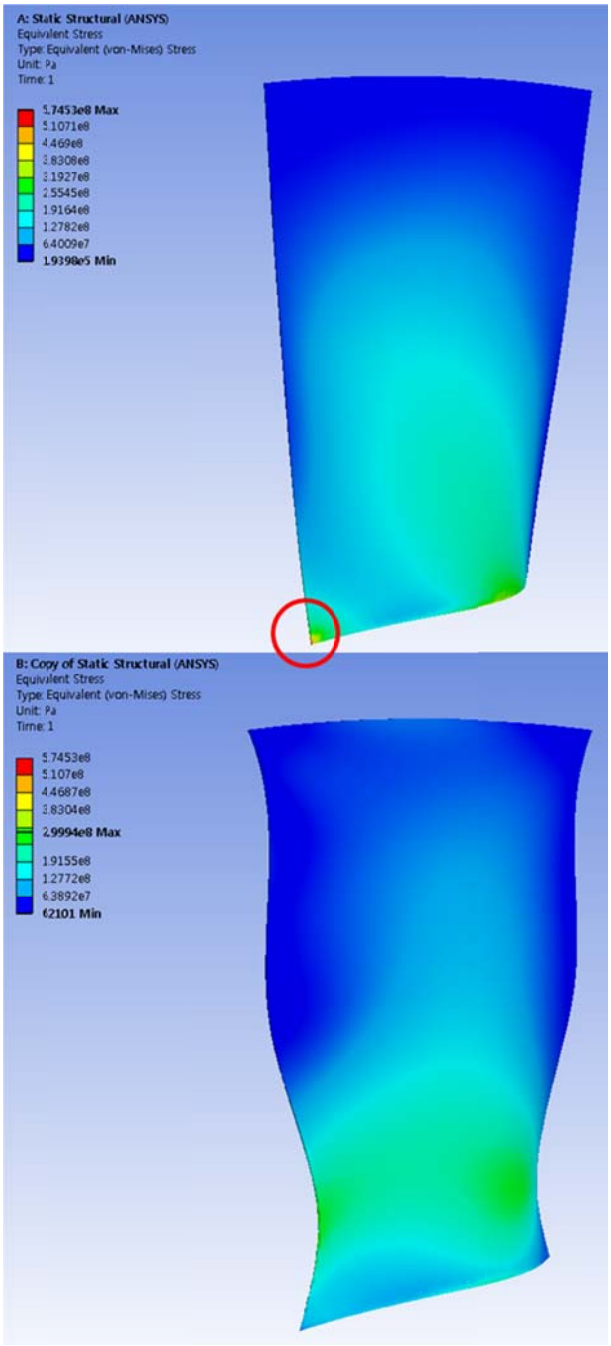

Fig. 4. 5 Contour of equivalent stress of baseline (upper) and optimized rotor (lower)

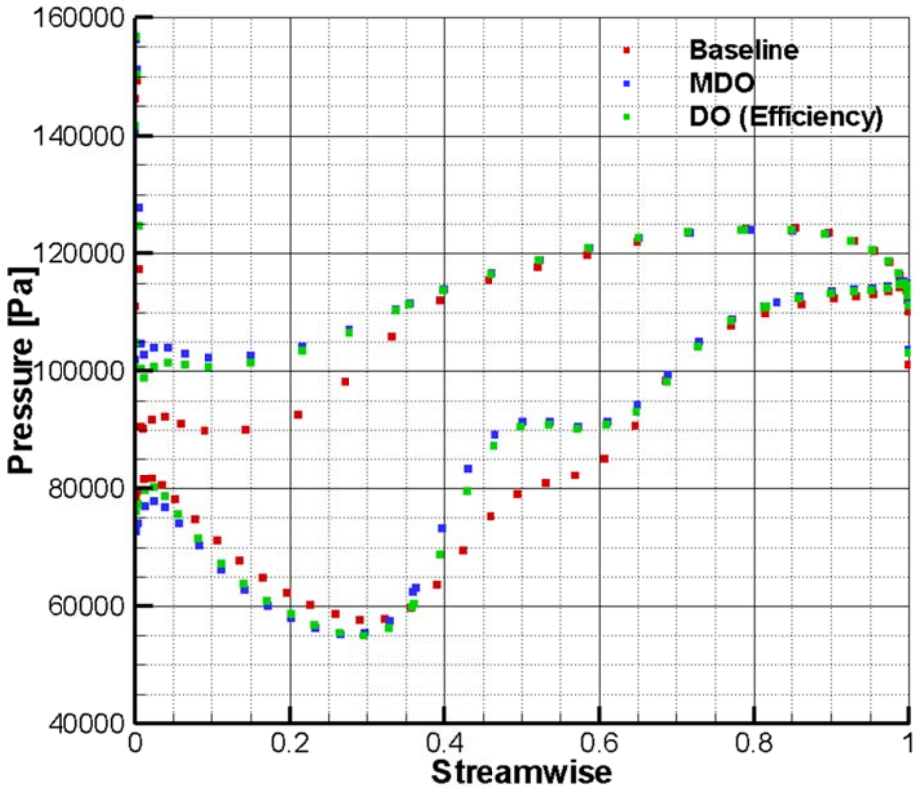

Fig. 4. 6 Blade Loading at 25% Span Length

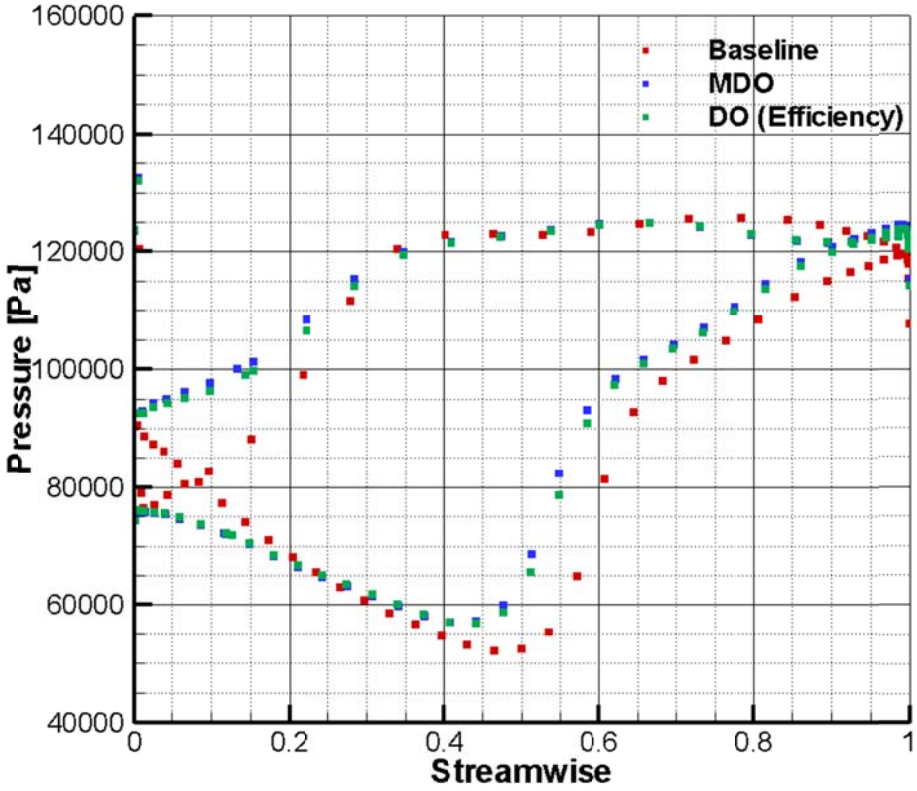

Fig. 4. 7 Blade Loading at 50% Span Length

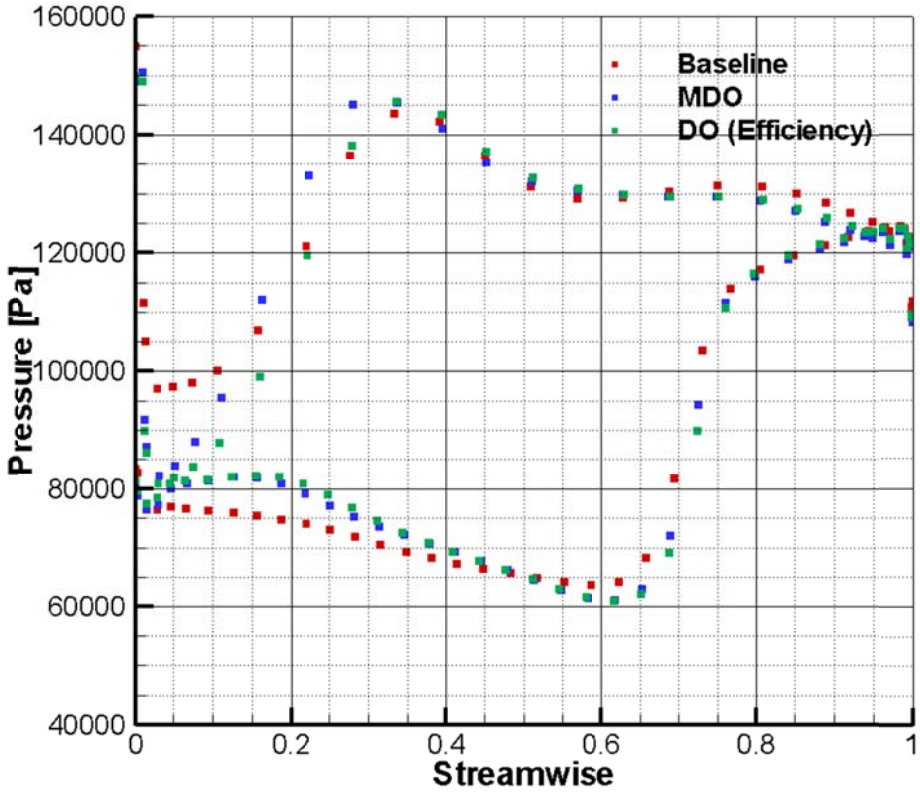

Fig. 4. 8 Blade Loading at 98% Span Length

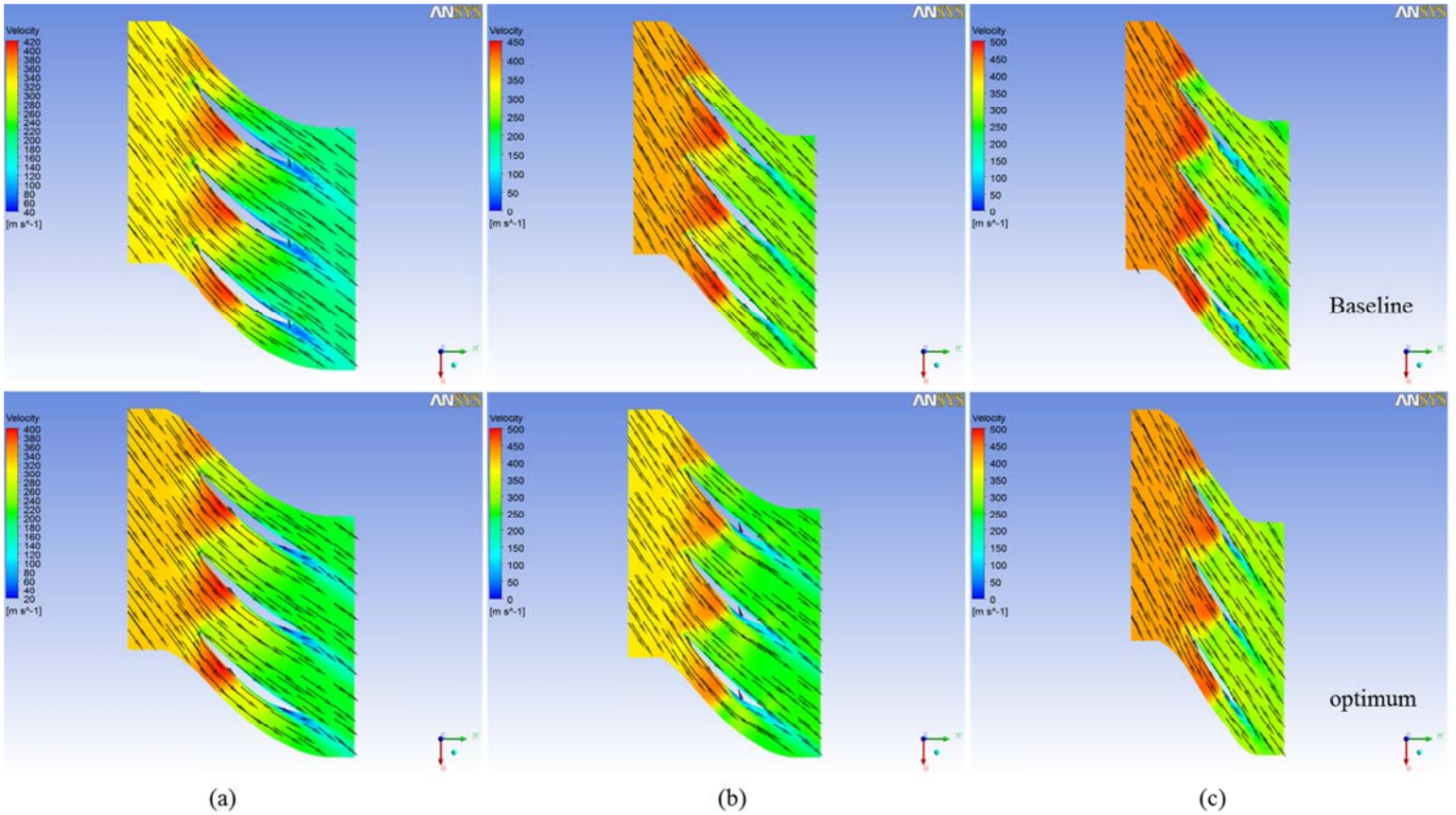

Fig. 4. 9 Mach number contour with velocity vector at (a) 20%, (b) 50%, (c) 80% span

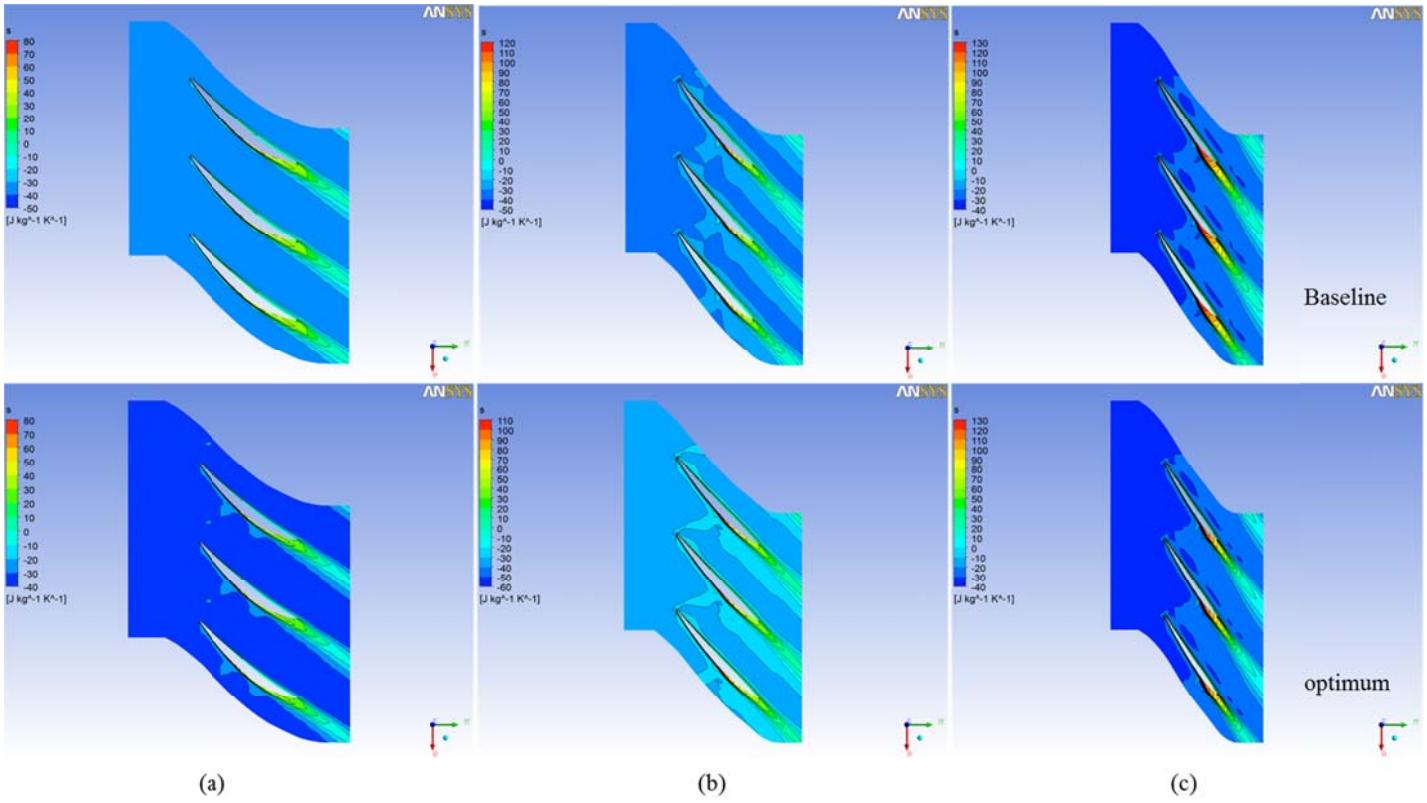

Fig. 4. 10 Entropy contour at (a) 20%, (b) 50%, (c) 80% span

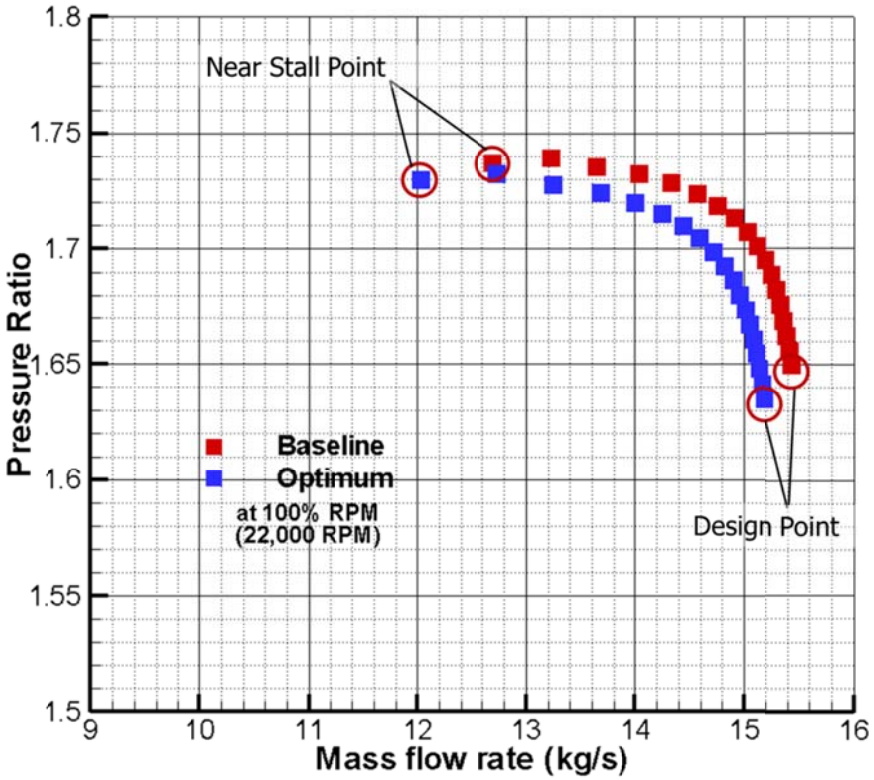

Fig. 4. 11 The working map of the rotor blades at 100% rotation speed

Chapter 5. Conclusion

In this study, a compressor MDO process with multi-step optimization was developed to increase the reliability. 60 design parameters were chosen for the rotor optimization and the stator was redesigned according to the rotor outlet flow angle variation to match the stator incidence angle by -1~0 degrees. To obtain the maximum value of the objective function, defined with the normalized isentropic efficiency and the safety factor of the compressor, a double-step optimization technique was adopted to minimize error between the MDO method and the numerical simulation results.

The CFD and FEA results showed an improvement of the isentropic efficiency and safety factor values that are within the allowable error bounds. The CFD results showed that the optimized rotor has more blade fore-load and relieved aft-load to reduce the flow detachment at the hub trailing edge. And more blade loading is burden to the hub region by increasing the incidence angle. The fore part blade loading gradually decreases along the span-wise direction by decreasing the rotor incidence angle. On the other hand, the tip chord length becomes longer and shock discontinuity point is relocated to coincide with the blade leading edge in the optimized rotor. For this reason, the rotor tip experiences lesser steep increase in the blade loading in the optimized rotor. In addition, relocation of the shock results in appropriate blade loading near the blade leading edge. Also the optimized stator has improved flow condition near the hub and shroud, which results in the efficiency gain of the compressor. The FEA results showed that the long first section chord and the relatively short second section chord form a trapezoid shape near the hub. This results in drastic stress relief at the blade hub. The final design achieved efficiency gain of 3.69% and showed a higher safety

factor by 2.2 times relative to the baseline model, while maintaining its stage mass flow rate and total-to-total pressure within the design constraints. The full-scaled compressor rig test data indicate that the overall aerodynamic performances agree well with the optimization and CFD results.

MDO with diffusion factor was done in chapter 4. The result shows that efficient performance with stable working area. The adiabatic efficiency is grown by 4.49% than the baseline. And the diffusion factor is decreased by 4.30%. The diffusion factor decreases the separation area near the trailing edge region and moves the shock wave to the rotor inlet to minimize the shock losses. As the diffusion factor is decreased, the stall margin is increased by 19.7% than the baseline result.

With results of chapter 3 and 4, kriging model shows better performance than ANN model to imitate the real design space with same experiment points. And it is confirmed that the stable working area can be extended with controlling the diffusion factor.

Validation for the increased stall margin in chapter 4 is can be a future works. It can approve the relation between the modified diffusion factor and the stall margin. It can suggest an interesting new design direction and meaningful results.

References

[1] Ki-Sang Lee, Kwang-Yong Kim, and Abdus Samad, “Design optimization of low-speed axial flow fan blade with three-dimensional RANS analysis”, Journal of Mechanical Science and Technology, Vol. 22 No.10, 2008, pp. 1864-1869

[2] Erneto Benini, “Three-Dimensional Multi-Objective Design Optimization of a Transonic Compressor Rotor”, Journal of Propulsion and Power, Vol.20, No.3, 2004, pp. 559-565

[3] Abdus Samad and Kwang-Yong Kim, “Multi-objective optimization of an axial compressor blade”, Journal of Mechanical Science and Technology, Vol.22, No.5, 2008, pp. 999-1007

[4] Kyoung-Yong Lee, Young-Seok Choi, Young-Lyul Kim, and Jae-Ho Yun, “Design of axial fan using inverse design method”, Journal of Mechanical Science and Technology, Vol.22, No.10, 2008, pp. 1883-1888

[5] Akin Keskin and Dieter Bestle, Application of multi-objective optimization to axial compressor preliminary design, Aerospace Science and Technology, Vol.10, No.7, 2006, pp. 581~589

[6] Lingen Chen, Jun Luo, Fengrui Sun, and Chih Wu, “Design efficiency optimization of one-dimensional multi-stage axial-flow compressor”, Applied Energy Vol.85, 2008, pp. 625-633

[7] Jae-Ho Choi, “A Study on Centrifugal Compressor Design Optimization for Increasing Surge Margin”, Journal of Fluid Machinery, Vol.11, No.2, 2008, pp. 38-45

[8] V.-M.Lei, Z.S.Spakovszky, E.M.Greitzer, “A Criterion for Axial Compressor Hub-Corner Stall”, Journal of Turbomachinery, Vol. 130, No.3, 2008, 031006. 1-10

[9] Kai Becker, Martin Lawerenz, Christian Voss, Reinhard Moenig, “Multi-Objective Optimization in Axial Compressor Design using a Linked CFD-Solver”, Proceedings of ASME Turbo Expo 2008: Power for Land, Sea and Air (GT2008), Berlin, Germany, 2008

[10] Christoph Leyens, Frank Kocian, Joachim Hausmann, and Wolfgang A. Kaysser, “Materials and design concepts for high performance compressor components”, Aerospace Science and Technology, Vol.7, No.3, 2003, pp. 201-210

[11] Jin Shik Lim and Myung Kyoon Chung, “Design point optimization of an axial-flow compressor stage”, International Journal of Heat and Fluid Flow, Vol. 10, No.1, 1989, pp. 48-58

[12] Yongsheng Lian and Meng-Sing Liou, “Multiobjective Optimization Using Coupled Response Surface Model and Evolutionary Algoorithm”, AIAA Journal, Vol.43, No.6, 2005, pp. 1316-1325

[13] S. Pierret, R. Filomeno Coelho, and H. Kato, “Multidisciplinary and multiple operating points shape optimization of three-dimensional compressor blades”, Structural and Multidisciplinary Optimization, Vol.33, No.1, 2007, pp. 61-70

[14] Akira Oyama and Meng-Sing Liou, “Multiobjective Optimization of Rocket Engine Pumps Using Evolutionary Algorithm”, Journal of Propulsion and Power, Vol.18, No.3, 2002, pp. 528-535

[15] Sangwon Hong, Hyungmin Kang, Saeil Lee, Sangook Jun, Dong-Ho Lee, Young-Seok Kang and Soo-Seok Yang, “Multidisciplinary Design Optimization of Multi Stage Axial Compressor”, Journal of Fluid Machinery, Vol. 12, No. 5, 2009, pp. 72-78

[16] Sangwon-Hong, Saeil Lee, Sangook Jun, Dong-Ho Lee, Hyoungmin Kang, Young-Seok Kang and Soo-Seok Yang, “Reliability-based design

optimization of axial compressor using uncertainty model for stall margin", Journal of Mechanical Science and Technology, Vol. 25, No. 3, 2011, pp. 731-740

[17] Rolls-Royce plc., *The Jet Engine*, Technical Publications Department, Rolls-Royce, Derby, 1986, p.250

[18] Rolls-Royce plc., *The Jet Engine*, Technical Publications Department, Rolls-Royce, Derby, 1986, p.25

[19] Philip Hill and Carl Peterson, *Mechanics and Thermodynamics of Propulsion,* 2nd ed, Pearson, Reading, 1992, p.287

[20] N.A Cumpsty, *Compressor Aerodynamics*, Longman Scientific & Technical, Essex, 1989, p.3

[21] Ronald H.Aungier, *Axial-Flow Compressors*, ASME Press, New york, 2003, pp.20-21

[22] N.A Cumpsty, *Compressor Aerodynamics*, Longman Scientific & Technical, Essex, 1989, p.48

[23] Saeil Lee, Sun Choi, Changsoo Jeon, Young-Seok Kang, Soo-Seok Yang and Dong-ho Lee, "Multidisciplinary Design Optimization of Axial Compressor with Double Step Optimization", 8th AIAA Multidisciplinary Design Optimization Specialist Conference, AIAA 2012-1844.

[24] AxCent Help, Version 7.12.11.0, Concepts ETI Inc., Norwich, VM, 2008

[25] Yushin Kim, Yong-Hee Jeon, and Dong-Ho Lee, "Mult-Objective and Multidisciplinary Design Optimization of Supersonic Fighter Wing", Journal of Aircraft, Vol.43, No.3, 2006, pp. 817-824

[26] S. Pierret, "Multi-Objective Optimization of Three Dimensional Turbomachinery Blades", 1st European Conference for Aerospace Sciences, Moscow, Russia, 2005

[27] Michael G. Neubauer, William Watkins, and Joel Zeitlin, “D-Optimal Weighting Designs for Four and Five Objects”, The Electronic Journal of Linear Algebra, Vol.4, 1998, pp. 48-72

[28] Fabian Triefenbach, “Design of Experiments: The D-Optimal Approach and Its Implementation as a Computer Algorithm”, PhD thesis of UMEÅ University, Sweden, 2008

[29] Sangook Jun, Yong-Hee Jeon, Jeong-Hwa Kim, and Dong-Ho Lee, “Application of the Robust and Reliability-Based Design Optimization to the Aircraft Wing Design”, Journal of the Korean Society for Aeronautical and Space Science, Vol.34, No.8, 2006, pp. 24-32

[30] Yeong-Koung Kim, Young-Gyun Kim, Dong-Ho Lee, and Do Hyung Lee, 2002, “Application of Neural network to approximate design space”, Proceedings of the 2002 KSAS Spring Conference, 2002, pp. 297-300

[31] Seungon Kang, Sangook Jun, Kyung-Hyun Park, Yong-Hee Jeon, and Dong-Ho Lee, “Study of Neural Network Training Algorithm Comparison and Prediction of Unsteady Aerodynamic Forces of 2D Airfoil”, Journal of the Korean Society for Aeronautical and Space Science (KSAS), Vol.27, No.5, 2009, pp. 425-432

[32] Giunta, A. A, “Aircraft Multidisciplinary Design Optimization Using Design of Experiments Theory and Response Surface Modeling Methods,” Ph.D. thesis, Virginia Polytechnic Institute and State University, Balcksburg, VA, 1997

[33] Simpson, T. W., "A Concept Exploration Method for Product Family Design", Ph. D. Dissertation, 1998

[34] Ku, Y. C., “Verification of Feasibility of Design Space Using Response Surface and Kriging Method,” Master Thesis, Seoul National University, School of Mechanical and Aerospace Engineering, 2004

[35] Ku, Y. C., Jeon, Y. H., Kim, Y. S., Lee, D. H., “Improvement of the Design Space Feasibility Using the Response Surface and Kriging Method,” *Journal of the Korea Society for Aeronautical and Space Sciences*, Vol. 33, No. 2, 2005, pp. 32–38

[36] Jun, S. O., Jeon, Y. H., Kim, J. H., Lee, D. H., “Application of the Robust and Reliability-Based Design Optimization to the Aircraft Wing Design,” Journal of the Korea Society for Aeronautical and Space Sciences, Vol. 34, No. 8, 2006, pp. 24–32

[37] Vanderplaats, G. N., *Numerical Optimization Techniques for Engineering Design*, Vanderplaats Research & Development, Inc., pp. 241-244, 320-325, 1999

[38] Vanderplaats, G. N., Hansen, S. R., *DOT USER MANUAL*, VMA Engineering, 1989

[39] Ernesto Benini, Roberto Biollo, “Aerodynamics of swept and leaned transonic compressor-rotors”, Applied Energy, Vol.84, No.10, 2007, pp.1012-1027.

[40] H. D. Céron-Muñoz, R. Cosin, R. F. F. Coimbra, L. G. N. Correa, and F. M. Catalano. "Experimental Investigation of Wing-Tip Devices on the Reduction of Induced Drag", Journal of Aircraft, Vol. 50, No. 2, 2013, pp. 441-449

[41] ANSYS TurboGrid User Manual, Version 13.0, ANSYS Inc., Canonsburg, PA, 2010

[42] Stefan Reh, Jean-Daniel Beley, Siddhartha Mukherjee, and Eng Hui Khor, “Probabilistic finite element analysis using ANSYS”, Structural Safety, Vol.28, 2006, pp. 17-43

[43] Joo Ho Choi, “Shape Design Sensitivity Analysis of Thermal Conduction Problems using Commercial Software ANSYS”, The Korean

Society of Mechanical Engineers, Transactions of the Korean Society of Mechanical Engineers-A, Vol.24, No.3, 2000, pp. 645-652

[44] Swapan Kumar Nandi, “Finite Element Analysis for Acoustic Behavior of a Refrigeration Compressor”, 2004 International ANSYS Conference Proceedings, Pittsburgh, Pennsylvania, USA, 2004

[45] Kelly Eberle and Chris Harper, “Dynamic Analysis of Reciprocating Compressors on FPSO Topside Modules”, 5th Conference of the EFRC, Prague, Czech, 2007

[46] T. G. Park, I. S. Jung, H. T. Jung, J. Y. Park, S. M. Kim, and J. H. Baek, “Numerical Investigation of the Effect of the Stagger Angle on the Aerodynamic Performance in the Vaned Diffuser of a Centrifugal Compressor”, Journal of computational fluids engineering, Vol.15, No.3, 2010, pp. 60-65

[47] Sang-Joon Yoon, Seok-Ho Son, and Dong-Hoon Cho, “Head Slider Designs Considering Dynamic LUL Systems for 1-in Disk Drives”, IEEE Transactions on Magnetics, Vol.44, No.1, 2008, pp. 151-156

[48] Jong-Rip Kim, Dong-Hoon Choi, “Enhanced two-point diagonal quadratic approximation methods for design optimization”, Computer methods in applied machanics and engineering, Vol.197, 2008, pp. 846-856

[49] B. L. Choi, D. H. Choi, J. Min, K. Jeon, J. Park, S. Choi, and J. M. Ko, “Torsion Beam Axle System Design With a Multidisciplinary Approach”, International Journal of Automotive Technology, Vol.10, No.1, 2009, pp. 49-54

[50] Chang-Hyun Park, Hee-jae Ahn, Dong-Hoon Choi, and Byung-Gi Pyo, “Two-Stage Design Optimization of an Automotive Fog Blank Cover for Enhancing Its Injection Molding Quality”, The Korean Society of

Mechanical Engineers, Transactions of the Korean Society of Mechanical Engineers-A, Vol.34, No.8, 2010, pp. 1097-1103

[51] Yushin Kim, Kwanjung Yee, and Dong-Ho Lee, “Aerodynamic Shape Design of Rotor Airfoils Undergoing Unsteady Motion”, Journal of Aircraft, Vol.41, No.2, 2004, pp. 247-257

[52] Zhen-Zhe Li, Yun-De Shen, Hui-Lan Xu, Jae-Woo Lee, Kwang-Su Heo, and Seoung-Yun Seol, “Optimal design of high temperature vacuum furnace using response surface method”, Journal of Mechanical Science and Technology, Vol.22, No.11, 2008, pp. 2213-2217

[53] Sangook Jun, Yong-Hee Jeon, Joohyun Rho, and Dong-ho Lee, “Application of Collaborative Optimization Using Genetic Algorithm and Response Surface Method to an Aircraft Wing Design”, Journal of Mechanical Science and Technology, Vol.20, No.1, 2006, pp. 133-146

[54] Christian Voβ, Marcel Aulich, Burak Kaplan and Eberhard Nicke, “Automated multiobjective optimization in axial compressor blade design”, Proceedings of ASME Turbo Expo 2006: Power for Land, Sea and Air (GT2006), Barcelona, Spain, 2006

[55] Korea Aerospace Research Institute, *Final Report of Development of Multidisciplinary Integrated Technology for Small High Loaded Compressor*, KATRA, 2012

[56] K.L. Suder, M.D. Hathaway, S.A. Thorp, A.J. Strazisar and M.B. Bright, "Compressor Stability Enhancement Using Discrete Tip Injection”, Journal of Turbomachinery, Vol.123, No.1, 2001, pp. 14-23

[57] H. Khaleghi, J.A. Teixeira, A.M. Tousi and M. Boroomand, “Parametric Study of Injection Angle Effects on Stability of Transonic Axial Compressors”, Journal of Propulsion and Power, Vol. 24, No. 5, 2008, pp.

1100-1107

[58] Hyun-Hoo Lee, Sung-Jong Kim, and Sang-Kwon Lee, “Design of new sound metric and its application for quantification of an axle gear whine sound by utilizing artificial neural network”, Journal of Mechanical Science and Technology, Vol.23, No.4, 2009, pp. 1182-1193

초 록

본 연구에서는 항공기용 저압 축류 압축기의 실 제작에 활용할 수 있을 정도의 신뢰성을 가진 공력/구조 최적설계를 위하여 근사모델을 이용하여 전역 최적해를 확보하고 근사모델에 내재된 오차의 영향을 없애기 위해 탐색된 최적해로부터 매 단계마다 해석을 수행하여 다시 한번 해를 찾는 다단계 최적설계(Double Step Optimization)에 대해서 제안하였다. 먼저 근사모델을 이용하여 압축기의 최적 형상을 도출하는 항공기용 축류 압축기 최적설계 프레임워크를 구축한 후 정해진 최적 형상의 수치해석적 공력 성능과 이를 기반으로 만든 실험 모델의 공력성능을 비교하여 프레임워크의 신뢰도를 검증하였다. 그 후 근사모델에서 발생하는 오차가 이미 축적된 설계 노하우와 반복적인 개선을 통하여 어느 정도 성능을 확보한 기본 형상에 대한 최적해의 성능 향상에 비해 무시할 만한 크기가 아니기 때문에 이를 해결하기 위해 어느 정도 전역 최적해를 확보한 후 기울기 기반 탐색기법을 이용해 매 탐색단계마다 해석을 수행하는 기법을 적용하였다. 인공 신경망을 이용하여 근사모델을 구축한 후 최적화를 진행하였고, 그 결과 공력 효율은 약 3.7% point, 구조 목적함수인 안전계수는 약 217%가 증가함을 볼 수 있었다.

또한 본 연구에서는 작동점만을 고려한 최적설계의 경우 스톨 마진을 확보할 수가 없기 때문에 안정적인 작동 영역을 확보하기

위해 확산 인자(Diffusion Factor)를 이용하여 손실을 저감하며 마진 확보를 할 수 있도록 하였다. 확산 인자는 임계 확산 인자보다 작아야 하므로 공력 효율은 최대화 하면서 확산 인자는 최소화 하는 방향으로 최적화를 진행하였다. 근사 모델은 크리깅 모델을 이용하여 구축하였고 진화 알고리즘을 이용하여 최적해를 구하였다. 그 결과 공력 효율은 약 4.5%, 안전계수는 약 14.6% 가량 증가하면서 확산 인자도 4.4% 가량 감소시키는 결과를 얻었다. 확산 인자가 감소함에 따라 스톨 마진은 19.7% 정도 보다 더 확보되었다. 따라서 본 연구에서 제안된 다단계 최적설계 기법을 항공기용 축류 압축기 최적설계에 적용할 경우 설계의 정확성은 확보하면서 성능 또한 상당히 개선된 결과를 얻을 수 있음을 확인할 수 있었다.

주요어: Multidisciplinary Design Optimization, Transonic Axial Low Pressure Compressor, Approximation Model, Double Step Optimization, Gradient Based Method, Stall Margin.

학 번 : 2009-20706

성 명 : 이 세 일

Appendix

Table A.1 Design of experiment data for efficiency and safety factor of objective function at 129 experiment points by D-Optimal design

No.	x_1	x_2	x_3	x_4	x_5	x_6	x_7	x_8	x_9	x_{10}	Nor.Eff	Nor.SF
1	-1	-1	-1	-1	-1	-1	1	-1	-1	-1	0.993	1.295
2	-1	-1	-1	-1	-1	1	-1	-1	1	-1	0.988	1.304
3	-1	-1	-1	-1	-1	1	0	1	-1	1	1.001	1.386
4	-1	-1	-1	-1	-1	1	1	-1	1	0	0.997	1.355
5	-1	-1	-1	-1	1	-1	-1	1	1	-1	0.996	1.010
6	-1	-1	-1	-1	1	-1	1	0	0	1	0.992	1.113
7	-1	-1	-1	-1	1	0	-1	-1	-1	-1	1.014	0.846
8	-1	-1	-1	1	-1	-1	-1	1	-1	-1	0.980	0.979
9	-1	-1	-1	1	-1	-1	1	-1	1	-1	0.985	1.152
10	-1	-1	-1	1	0	1	-1	-1	-1	1	0.988	0.963
11	-1	-1	-1	1	1	-1	-1	-1	1	0	0.987	0.949
12	-1	-1	-1	1	1	1	-1	1	1	1	0.993	0.922
13	-1	-1	-1	1	1	1	1	1	-1	-1	0.990	1.053
14	-1	-1	0	-1	-1	-1	-1	-1	-1	1	0.997	1.324
15	-1	-1	0	0	1	1	0	-1	1	-1	0.998	0.988
16	-1	-1	0	1	-1	1	0	1	1	-1	0.991	1.053
17	-1	-1	1	-1	-1	-1	1	1	1	1	0.995	1.372
18	-1	-1	1	-1	-1	1	-1	1	-1	-1	0.992	1.302
19	-1	-1	1	-1	1	1	-1	-1	1	1	1.000	0.969
20	-1	-1	1	-1	1	1	1	1	1	-1	0.996	1.088
21	-1	-1	1	0	1	-1	0	1	-1	0	0.998	1.015
22	-1	-1	1	1	-1	0	-1	1	1	1	0.990	0.944
23	-1	-1	1	1	-1	1	1	-1	-1	-1	0.989	1.119
24	-1	-1	1	1	1	-1	-1	-1	-1	-1	0.986	0.953
25	-1	-1	1	1	1	-1	1	-1	1	1	0.989	1.044

26	-1	-1	1	1	1	0	1	1	0	1	0.991	1.031
27	-1	0	-1	-1	1	1	1	-1	-1	1	0.997	1.236
28	-1	0	-1	0	-1	-1	-1	0	0	0	0.992	1.043
29	-1	0	-1	1	-1	1	1	1	1	1	0.993	1.014
30	-1	0	1	1	-1	1	-1	-1	1	0	0.983	0.937
31	-1	0	1	1	1	-1	-1	1	-1	1	0.991	0.871
32	-1	1	-1	-1	-1	-1	-1	1	-1	1	1.003	1.130
33	-1	1	-1	-1	-1	1	-1	-1	1	1	1.003	1.153
34	-1	1	-1	-1	0	1	1	1	0	0	1.002	0.921
35	-1	1	-1	-1	1	-1	0	1	1	1	1.004	1.294
36	-1	1	-1	-1	1	-1	1	-1	1	-1	0.998	1.248
37	-1	1	-1	-1	1	1	-1	1	-1	-1	1.000	1.191
38	-1	1	-1	1	-1	0	1	1	-1	-1	0.987	0.977
39	-1	1	-1	1	-1	1	-1	-1	-1	-1	0.976	0.891
40	-1	1	-1	1	1	-1	1	-1	-1	1	0.985	0.981
41	-1	1	-1	1	1	0	-1	-1	1	-1	0.982	0.852
42	-1	1	-1	1	1	1	1	-1	1	1	0.991	0.982
43	-1	1	0	1	-1	-1	1	-1	-1	1	0.986	0.961
44	-1	1	0	1	0	-1	-1	0	1	1	0.989	0.851
45	-1	1	1	-1	-1	-1	-1	1	1	1	1.004	1.126
46	-1	1	1	-1	-1	-1	1	1	-1	-1	1.000	1.268
47	-1	1	1	-1	-1	1	1	-1	-1	1	1.001	1.052
48	-1	1	1	-1	-1	1	1	0	1	-1	1.003	1.232
49	-1	1	1	-1	0	-1	-1	-1	0	-1	0.998	1.198
50	-1	1	1	-1	1	-1	-1	-1	-1	1	1.004	1.152
51	-1	1	1	-1	1	1	1	1	-1	1	0.999	1.244
52	-1	1	1	0	-1	0	1	-1	1	1	0.999	1.145
53	-1	1	1	1	-1	-1	-1	-1	1	-1	0.980	0.880
54	-1	1	1	1	-1	1	-1	1	-1	1	0.991	0.850
55	-1	1	1	1	1	-1	1	1	1	-1	0.990	0.963
56	-1	1	1	1	1	1	-1	1	1	-1	0.987	0.841
57	-1	1	1	1	1	1	1	-1	-1	-1	0.994	0.814

58	0	-1	-1	0	0	-1	1	1	-1	1	0.990	0.981
59	0	-1	-1	1	1	1	1	0	1	-1	0.989	1.091
60	0	-1	1	-1	1	1	-1	1	1	1	0.989	0.799
61	0	-1	1	0	-1	1	1	1	-1	1	1.002	0.873
62	0	0	-1	1	-1	-1	0	-1	0	1	0.995	1.154
63	0	0	0	-1	-1	0	1	1	1	-1	0.983	1.043
64	0	0	0	0	0	0	0	0	0	0	1.000	1.000
65	0	0	1	-1	1	-1	0	-1	1	1	0.996	1.179
66	0	1	-1	-1	-1	1	-1	1	1	-1	1.002	1.053
67	0	1	-1	1	1	-1	-1	1	0	1	0.998	1.139
68	0	1	0	-1	1	-1	1	0	-1	-1	0.986	0.888
69	0	1	1	1	-1	-1	1	1	1	0	0.997	0.889
70	0	1	1	1	0	0	0	-1	-1	0	0.988	1.048
71	1	-1	-1	-1	-1	-1	-1	0	-1	-1	0.987	0.971
72	1	-1	-1	-1	-1	1	1	1	-1	-1	0.989	0.809
73	1	-1	-1	-1	1	-1	-1	1	-1	1	0.995	0.802
74	1	-1	-1	-1	1	1	0	-1	0	-1	0.995	0.814
75	1	-1	-1	-1	1	1	1	1	1	1	0.996	0.716
76	1	-1	-1	0	-1	1	-1	1	1	-1	0.995	0.724
77	1	-1	-1	0	1	-1	-1	-1	1	1	0.984	0.962
78	1	-1	-1	1	-1	-1	0	1	1	1	0.990	0.916
79	1	-1	-1	1	-1	0	1	-1	1	1	0.982	0.972
80	1	-1	-1	1	-1	1	-1	-1	-1	-1	0.969	1.002
81	1	-1	-1	1	1	-1	1	-1	-1	-1	0.976	0.804
82	1	-1	-1	1	1	1	-1	1	-1	0	0.983	0.936
83	1	-1	0	1	-1	-1	1	1	-1	0	0.979	0.936
84	1	-1	0	1	1	1	1	-1	-1	1	0.983	0.893
85	1	-1	1	-1	-1	-1	-1	1	0	1	0.996	0.864
86	1	-1	1	-1	-1	-1	0	-1	1	-1	0.994	0.799
87	1	-1	1	-1	-1	1	1	-1	1	1	0.997	0.809
88	1	-1	1	-1	1	-1	1	-1	-1	1	0.991	0.724
89	1	-1	1	-1	1	-1	1	1	0	-1	0.992	0.705

90	1	-1	1	-1	1	1	-1	-1	-1	-1	0.994	0.814
91	1	-1	1	1	-1	-1	-1	-1	-1	1	0.979	0.992
92	1	-1	1	1	-1	-1	1	0	1	-1	0.981	0.967
93	1	-1	1	1	0	0	-1	1	-1	-1	0.979	0.960
94	1	-1	1	1	0	1	1	1	1	1	0.987	0.910
95	1	-1	1	1	1	-1	-1	1	1	1	0.987	0.954
96	1	-1	1	1	1	1	-1	-1	1	-1	0.980	0.945
97	1	-1	1	1	1	1	0	0	-1	1	0.989	0.930
98	1	0	-1	-1	0	-1	-1	-1	1	-1	0.982	0.882
99	1	0	-1	1	1	-1	1	1	1	-1	0.979	0.973
100	1	0	0	-1	0	1	-1	1	-1	1	0.981	0.950
101	1	0	1	0	-1	-1	1	-1	-1	-1	0.979	0.977
102	1	0	1	1	-1	-1	1	0	-1	1	0.987	0.928
103	1	1	-1	-1	-1	-1	-1	-1	-1	0	0.987	0.940
104	1	1	-1	-1	-1	-1	1	-1	1	1	0.980	0.766
105	1	1	-1	-1	-1	-1	1	1	1	-1	0.989	0.841
106	1	1	-1	-1	-1	1	1	-1	-1	1	0.992	0.842
107	1	1	-1	-1	1	-1	0	1	-1	-1	0.979	0.875
108	1	1	-1	-1	1	1	-1	-1	1	1	1.000	0.845
109	1	1	-1	0	0	1	1	0	-1	-1	0.988	0.856
110	1	1	-1	1	-1	-1	-1	1	1	1	0.979	0.935
111	1	1	-1	1	-1	1	-1	1	-1	1	0.995	0.852
112	1	1	-1	1	-1	1	1	-1	1	-1	0.998	0.755
113	1	1	-1	1	1	-1	-1	-1	-1	1	0.999	0.756
114	1	1	-1	1	1	1	-1	1	1	-1	1.000	0.746
115	1	1	-1	1	1	1	1	1	-1	1	1.035	0.657
116	1	1	0	0	1	0	1	1	1	1	1.003	0.811
117	1	1	0	1	1	-1	-1	-1	0	-1	0.991	0.790
118	1	1	1	-1	-1	1	-1	-1	-1	-1	0.980	0.913
119	1	1	1	-1	-1	1	0	1	1	1	0.981	0.919
120	1	1	1	-1	0	-1	1	1	-1	1	0.983	0.926
121	1	1	1	-1	1	-1	-1	1	1	-1	0.980	0.908

122	1	1	1	-1	1	0	-1	0	1	0	0.980	0.904
123	1	1	1	-1	1	1	1	-1	1	-1	0.981	0.873
124	1	1	1	0	1	1	-1	-1	-1	1	0.993	0.790
125	1	1	1	1	-1	-1	-1	1	-1	-1	0.977	0.914
126	1	1	1	1	-1	1	-1	-1	1	1	0.994	0.827
127	1	1	1	1	-1	1	1	1	0	-1	1.006	0.805
128	1	1	1	1	1	-1	1	-1	1	1	0.982	0.874
129	1	1	1	1	1	1	1	1	-1	-1	0.984	0.865